Preparation and optimization of agarose or polyacrylamide/amino acid-based double network hydrogels for photocontrolled drug release

Shunyu Xiang, Chloé Guilbaud-Chéreau, Paul Hoschtettler, Loïc Stefan, Alberto Bianco, Cécilia Ménard-Moyon

Preparation and optimization of agarose or polyacrylamide/amino acid-based double network hydrogels for photocontrolled drug release

Shunyu Xiang[1], *Chloé Guilbaud-Chéreau*[1], *Paul Hoschtettler*[2], *Loïc Stefan*[2], *Alberto Bianco*[1,*], *Cécilia Ménard-Moyon*[1,*]

[1]CNRS, Immunology, Immunopathology and Therapeutic Chemistry, UPR 3572, University of Strasbourg, ISIS, 67000 Strasbourg, France

[2]Université de Lorraine, CNRS, LCPM, 54000 Nancy, France

* Corresponding Authors: c.menard@ibmc-cnrs.unistra.fr, a.bianco@ibmc-cnrs.unistra.fr

Abstract

The high water content and biocompatibility of amino-acid-based supramolecular hydrogels have generated growing interest in drug delivery research. Nevertheless, the existing dominant approach of constructing such hydrogels, the exploitation of a single amino acid type, typically comes with several drawbacks such as weak mechanical properties and long gelation times, hindering their applications. Here, we design a near-infrared (NIR) light-responsive double network (DN) structure, containing amino acids and different synthetic or natural polymers, *i.e.*, polyacrylamide, poly(*N*-isopropylacrylamide), agarose, or low-gelling agarose. The hydrogels displayed high mechanical strength and high drug-loading capacity. Adjusting the ratio of Fmoc-Tyr-OH/Fmoc-Tyr(Bzl)-OH or Fmoc-Phe-OH/Fmoc-Tyr(Bzl)-OH, we could drastically shorten the gelation time of the DN hydrogels at room and body temperatures. Moreover, introducing photothermal agents (graphene oxide, carbon nanotubes, molybdenum disulfide nanosheets, or indocyanine green), we equipped the hydrogels with NIR responsivity. We demonstrated the light-triggered release of the drug baclofen, which is used in severe spasticity treatment. Rheology and stability tests confirmed the positive impact of the polymers on the mechanical strength of the hydrogels, while maintaining good stability under physiological conditions. Overall, our study contributed a novel hydrogel formulation with high mechanical resistance, rapid gel formation, and efficient NIR-controlled drug release, offering new opportunities for biomedical applications.

Keywords: baclofen, carbon nanomaterials, molybdenum disulfide, photothermal agents, poly(*N*-isopropylacrylamide), self-assembly.

1. Introduction

Severe spasticity is a symptom characteristically observed in various neurological disorders, generally causing excruciating pain and associated with several secondary complications [1]. Currently, the reference treatment for severe spasticity is the continuous intrathecal infusion of baclofen, which is an effective yet highly invasive and costly mode of administration [2]. In recent years, various delivery systems have been described for controlled and sustained release of baclofen [3-6]. Nevertheless, we still lack a rival for the intrathecal infusion, motivating us to explore alternative drug delivery platforms.

Owing to their high capacity and environmental responsivity, self-assembled hydrogels pose an effective tool for controlled drug release applications [7, 8]. Virtually countless structurally complex and functionally diverse compositions can be generated *via* molecular self-assembly, allowing unique potentials in biomedical applications including and beyond controlled drug delivery [8-10]. Among the possible compositions, low-molecular-weight supramolecular hydrogels often stand out owing to their excellent dynamic responsiveness, high water content, and superior biocompatibility [11-13]. Their formation is predominantly regulated by noncovalent interactions, such as electrostatic interactions, hydrogen bonding, van der Waals forces, and π-π stacking, often through driving the self-assembly of molecules into three-dimensional networks of entangled fibers [14]. Notably, such relatively weak interactions make low-molecular-weight supramolecular hydrogels sensitive to local environmental changes, such as temperature, pH, and mechanical stress, making them promising for controlled drug delivery purposes [15-17].

Recently, peptides and their derivatives have been widely investigated in designing biomedical supramolecular hydrogels, often because of their adjustable viscoelasticity, biocompatibility, and degradability [15,18-20]. Extensive research has focused on modulating the release behavior of drug-loaded hydrogels by varying pH, temperature, light, and ionic strength, as controlled by the peptide sequence (*i.e.*, the number and position of amino acids, and the introduction of chemical modifications) [19,21]. On another aspect, supramolecular hydrogels formed with peptides protected at the *N*-terminus with a fluorenylmethoxycarbonyl (Fmoc) group exhibited improved biocompatibility [22-26]. Fmoc-peptides can easily self-assemble in water to form fibrous hydrogels *via* intermolecular π-π stacking of the Fmoc group and hydrogen bonding between the amino acids [23]. However, peptide-based supramolecular hydrogels can lead to immunogenicity, inflammation, and, in severe cases, cytotoxicity [27,28]. In addition, peptide synthesis techniques are relatively complex and costly [27-29]. As a result, the widespread use of peptide-based supramolecular hydrogels is currently far from reality in drug delivery.

In contrast to peptide-based cases, amino-acid-based supramolecular hydrogels come with some critical advantages, such as their low cost, high biocompatibility, low cytotoxicity, low immunogenicity, and predictable degradation pathways [12,30,31]. Plus, similar to their peptide-based counterparts, amino-acid-based supramolecular hydrogels can be formed by the self-assembly of a single type of amino acid or co-assembly of different types [32]. In addition, this approach is instrumental in introducing additional functionalities to the developed hydrogels. For instance, the supramolecular hydrogels formed by the co-assembly of Fmoc-phenylalanine (gelation agent) and Fmoc-leucine (antimicrobial building block) showed superior antibacterial activity against

drug-resistant strains, without increasing mammalian toxicity [32]. Still, while amino-acid-based supramolecular hydrogels offer key advantages in drug delivery applications, there are various limitations to overcome. For example, the low mechanical strength of most amino-acid-based hydrogels can lead to premature dissolution or escape from the local delivery site [27,33]. Nevertheless, there is an effective strategy to improve the mechanical properties of amino-acid-based supramolecular hydrogels: integrating high-molecular-weight polymers in the self-assembled network, resulting in a dense structure often referred to as a double network (DN) [12,19,34,35].

In recent years, photo-responsive hydrogels have been considered ideal platforms for controlled drug delivery due to their photo-triggered release potential [36]. This strategy employs photothermal agents to convert light into heat that disrupts the equilibrium of the gel system or alters the internal structure of the gel, thereby controlling drug release [36]. Near-infrared (NIR) light can penetrate safely into tissues down to a few cm, making it an ideal choice for photocontrolled drug release [37]. We previously demonstrated that Fmoc-Tyr(Bzl)-OH/Fmoc-Tyr-OH and Fmoc-Tyr(Bzl)-OH/Fmoc-Phe-OH binary systems were able to form two hydrogels (named gel 1 and gel 2, respectively) [38]. The hydrogels were loaded with a photothermal agent (oxidized carbon nanotubes (CNTs) or graphene oxide (GO)) and a model drug (L-ascorbic acid), and they were able to release a high amount of drug under NIR light irradiation. Nevertheless, the applicability of those hydrogels for biomedical applications was hampered by their low mechanical stability. Thus, several strategies have been considered to improve their mechanical properties to create robust viscoelastic materials suitable for biomedical research. Among them, the development of DN hydrogels is of particular interest, thanks to their superb mechanical performance combining

both strength and toughness [39]. Interestingly, this unique balance can be finely tailored through the modulation of inter/intramolecular interactions and the structural composition of the two networks, playing with the chemical nature of the monomers and/or crosslinkers exploited [40,41]. Nevertheless, despite notable advancements made in the field, the applicability of DN hydrogels in drug delivery still encounters several challenges. For instance, many DN hydrogels lack of response to a specific external stimulus, which represents a major constraint for developing precise controlled drug delivery systems [42]. Also, the progress made in the use of DN hydrogels for photocontrolled drug release is still at an early stage, given that current systems do not allow low photothermal agent usage, precise drug release, and low laser power utilization [43]. Additionally, the complex synthetic steps involved in preparing most DN hydrogels limit their clinical applicability [44]. Consequently, only few scientific research reports exist to date on physicochemical crosslinked DN hydrogels, which are viscoelastic materials comprised of a noncovalent network combined with a covalent one [45,46], which is the primary focus of our work reported herein.

In the present work, we designed a straightforward procedure to prepare DN hydrogels by integrating a polymer network (agarose and polyacrylamide derivatives) in gel 1 and gel 2 to enhance their mechanical strength and shorten their gelation time, while maintaining their high photocontrolled drug release capacity. Agarose is a natural and FDA-approved polysaccharide, able to form a porous gel structure in aqueous media through noncovalent interactions like hydrogen bonds and electrostatic attractions [47]. The gelation of agarose is primarily driven by the formation of double helical structures within the agarose polymer chains. When heated, agarose mol-

ecules disperse in the liquid and remain in a solution state. As the temperature decreases, the agarose chains start to align and form helices due to intermolecular hydrogen bonding. These helices further aggregate and entangle to create a three-dimensional network structure, resulting in the formation of a gel. Agarose has gained attention in the materials science, particularly for designing DN hydrogels. Agarose-based DN hydrogels have been used for controlled drug release thanks to their capacity to provide a matrix for controlled diffusion of therapeutic agents [47]. Meanwhile, the mechanical properties of agarose-based DN hydrogels can be tailored by adjusting the concentration of agarose and thus the degree of chemical crosslinking in the second network, making agarose appealing for a wide range of applications, including tissue engineering and drug delivery [48]. Low-gelling agarose (2-hydroxyethyl agarose, named L-agarose) can also be used, as the chemical modification of agarose can govern the loading and release behavior of hydrogels [49]. Nevertheless, agarose-based hydrogels exhibit some limitations for drug delivery, such as low degradation rates, low adsorption potential for hydrophobic drug molecules and slow adsorption/desorption of some drugs [47,50,51]. However, there is evidence that mixing agarose with biomaterials or polysaccharides, such as sodium alginate and chitosan, can generate hydrogels with improved drug delivery potential compared to agarose gels [47,50,52,53].

In our work, the gel-to-sol transition of agarose hydrogels at a critical temperature may potentially improve the drug release characteristics of the amino acid hydrogels. Alternatively, acrylamides and modified acrylamides are common free radical polymerization monomers producing non-toxic polymers and hydrogels suitable for tissue engineering, drug delivery, and biosensing [54]. Besides, polyacrylamide (PAAm) hydrogels display many advantages, including

high stretchability, good biocompatibility, and simple synthesis [55], increasing their application potential as evidenced by clinical trials for their use in tissue regeneration or incontinence [56,57]. In addition, past studies have successfully employed PAAm-based DN hydrogels for controlled drug delivery applications, exploiting their capacity to swell/shrink in response to external stimuli, such as changes in pH or temperature for the controlled release of encapsulated drugs or therapeutic agents [54]. On the other hand, in addition to PAAm, we also exploited poly(*N*-isopropylacrylamide) (PNIPAAm), a prominent thermoresponsive polymer exhibiting highly reversible expansion and contraction behavior in response to temperature fluctuations [58], making it likely the most commonly used thermosensitive polymer for preparing drug-loaded hydrogels [59-61]. Notably, PNIPAAm-based hydrogels can undergo swelling and shrinking within the physiological temperature range, effectively promoting drug release [62]. Furthermore, the presence of PNIPAAm alters the gel phase transition temperature, consequently modulating the gel thermal responsiveness and ultimately enhancing the water and drug release performance [63]. Hence, the incorporation of PNIPAAm as a second network into gel 1 or gel 2 could allow for better control of the drug release thanks to the heat generated by the photothermal agents under NIR light irradiation. However, the weak mechanical properties, poor environmental responsiveness, and low drug-release ability of common PAAm and PNIPAAm hydrogels hinder their application potential in drug delivery [64,65]. At this point, introducing a secondary crosslinking network or adding a relatively rigid component, such as gelatin or a polysaccharide, into the PAAm or PNIPAAm hydrogels, appear to be effective strategies [56,64-67].

In this work, we combined PAAm, PNIPAAm, agarose, and L-agarose with gel 1 or gel 2 loaded with a photothermal agent, resulting in the formation of eight different DN hydrogels. The concentration of the polymerization initiators, namely ammonium persulphate (APS) and *N*,*N*,*N'*,*N'*-tetramethylethylenediamine (TEMED), was optimized to reduce the residual amount of acrylamide/*N*-isopropylacrylamide monomers. The hydrogels were characterized by nuclear magnetic resonance (NMR), Fourier-transform infrared (FTIR), and circular dichroism (CD) spectroscopies, as well as transmission electron microscopy (TEM). The gelation time was modulated by changing the ratio of Fmoc-Tyr-OH/Fmoc-Tyr(Bzl)-OH and Fmoc-Phe-OH/Fmoc-Tyr(Bzl)-OH. Rheological experiments and stability studies were performed to assess the mechanical properties of the DN hydrogels and their stability under physiological conditions. The DN hydrogels exhibited a high drug release capacity under NIR light irradiation, demonstrating their potential for precise and controlled drug release. Remarkably, low concentrations of PAAm and PNIPAAm were used (much lower compared to previous studies [68,69]), thereby ensuring not only the biocompatibility of the DN hydrogels, but also providing ample room to fine-tune their properties. Thus, overall, this work opens new avenues in designing baclofen-releasing hydrogels with implementations beyond drug delivery.

2. Experimental section

2.1. Materials and methods

Fmoc-Tyr(Bzl)-OH was purchased from Bachem, and Fmoc-Phe-OH and Fmoc-Tyr-OH were procured from PolyPeptide Group. 40% acrylamide/bis-acrylamide (37.5:1), *N*-isopropylacrylamide, agarose, L-agarose, TEMED, triethylene glycol dimethacrylate, baclofen, and RPMI-

1640 medium were purchased from Sigma-Aldrich, and ammonium persulphate and dimethyl sulfoxide (DMSO) were from Fisher Chemical. Dulbecco's Modified Eagle's Medium (DMEM) and fetal bovine serum were purchased from Lonza and Dominique Dutscher, respectively. Pristine multi-walled CNTs (20-30 nm diameter, 0.5-2 μm length, 95% purity; batch 1240XH) were purchased from Nanostructured and Amorphous Materials. The oxidation of CNTs was prepared according to our previous work [70]. GO was obtained from Grupo Antolin and molybdenum disulfide was from Acros Organics. The exfoliation of MoS_2 was carried out in an ethanol/water mixture [71], as described in the Supplementary Materials. Indocyanine green (ICG) was purchased from United States Pharmacopeia. The calibration curves of *N*-isopropylacrylamide, acrylamide and baclofen were assessed by HPLC (Nucleosil 100-5 Waters C18 reverse-phase HPLC column and Waters Alliance e2695 separation module) at 220 nm. The photothermal studies were performed using a NIR laser (808 nm) (Changchun New Industry Optoelectronics Technology Co., China), and the thermal imaging camera was a Flir One product (M/N: 0005).

2.2. Amino acid hydrogel preparation

Each Fmoc-protected amino acid was separately dissolved into DMSO at an initial concentration of 247 mM. Then, each Fmoc-protected amino acid solution was mixed at a ratio of 1:1, 1:1.5, or 1:2 and diluted with Milli-Q® water to a final concentration of 2.45:2.45, 2.45:3.7, 2.45:4.9 mM (Fmoc-Tyr-OH/Fmoc-Tyr(Bzl)-OH or Fmoc-Phe-OH/Fmoc-Tyr(Bzl)-OH). The solutions were sonicated in a water bath (Elmasonic P, 100 W, 37 kHz, Germany) for 10 s and left at room temperature. The gel formation was evidenced by the vial inversion test, *i.e.*, putting the vials upside down to see if the hydrogels are stable or not.

2.3. Polymer solution preparation

1. PAAm or PNIPAAm

Different amounts of 40% acrylamide/bis-acrylamide (or *N*-isopropylacrylamide/triethylene glycol dimethacrylate) were added into 10 mL of Milli-Q® water to prepare 1 wt%, 5 wt%, and 10 wt% acrylamide/bis-acrylamide (or *N*-isopropylacrylamide/triethylene glycol dimethacrylate) solutions (**Table S1**). Then, a 10 wt% APS solution was prepared, and 2% (v/v) APS and 0.2% (v/v) TEMED solutions were added in sequential order (optimized conditions). All mixed solutions were homogenized with a vortex mixer (Top-Mix 94323, Bioblock Scientific, Germany) for 30 s and left for 6 h to form PAAm (or PNIPAAm).

2. Agarose or L-agarose

10 mg of agarose or L-agarose were dissolved into 10 mL of Milli-Q® water and heated in an oil bath at 90 ℃ for 10 min. The agarose (or L-agarose) gel was obtained when the temperature was cooled down to room temperature.

2.4. Double network hydrogel preparation

The DN hydrogels were prepared in two steps:

1. Preparation of the amino acid solutions: 20 mg of baclofen and 2.55 mg of photothermal agent (GO, CNTs, ICG, or MoS_2 nanosheets) were added to 10 mL of Milli-Q® water to reach an initial concentration of 2 mg/mL and 225 μg/mL, respectively, and the suspension was sonicated in a water bath for 3 min. Then, 480 μL of the baclofen/photothermal agent solution/dispersion was mixed with 20 μL of the amino acid binary solution prepared following the protocol reported in Section 2.2.

2. Addition of the PAAm, PNIPAAm, agarose, or L-agarose solutions: Firstly, the PAAm, PNIPAAm, agarose and L-agarose solutions were prepared according to the protocol reported in Section 2.3. Then, 500 μL of PAAm, PNIPAAm, agarose, or L-agarose solution were mixed with the amino acid solution (500 μL). The resulting solution was mixed three times using a micropipette.

2.5. NMR spectroscopy

The hydrogels were freeze-dried for 24 h using a lyophilizer (Cryotec, France). The dried samples were solubilized in D_2O, and the solution was transferred into an NMR tube. Finally, ^1H liquid-state NMR spectra were recorded in $CDCl_3$ using a Bruker Avance III 400 MHz. MestReNova was used to analyze the NMR data and measure the integrated area of the monomers (acrylamide: 6.10 and 5.72 ppm; *N*-isopropylacrylamide: 6.05 and 5.66 ppm) and polymers (PAAm: 2.13 and 1.57 ppm; PNIPAAm: 1.94 and 1.49 ppm) in the DN hydrogels.

2.6. FTIR spectroscopy

FTIR analysis was performed using a PerkinElmer Frontier™ FTIR spectrometer. The dried hydrogel samples were placed on the attenuated total reflectance detector and measured under ambient conditions (number of scans: 64).

2.7. Transmission electron microscopy

TEM analysis was done using a Hitachi 7500 transmission electron microscope (Hitachi High Technologies Corporation, Japan) equipped with an AMT Hamamatsu digital camera (Hamamatsu Photonics, Japan) at an accelerative voltage of 80 kV. To prepare the samples, a volume of 1 mL of hydrogel was shaken to allow taking 10 μL, which were deposited onto a carbon-coated copper

grid (Formvar/Carbon 300 Mesh, Cu from Delta Microscopies). The grids were dried under a fume hood before observation. The width of the amino acid fibrils was measured using Nano Measurer 1.2 software.

2.8. Circular dichroism

Circular dichroism analysis was performed using a JASCO J-810 spectropolarimeter (JASCO, Japan). First, 1 mL of the solution of amino acids or amino acid mixtures (2.45:3.7 mM) and polymers (1% PAAm or PNIPAAm; 0.1% agarose or L-agarose) was diluted 20 times and transferred to a 1 mm pathlength quartz cuvette. The CD analyses were performed directly after the dilution and after 1 h (from 350 to 190 nm, 100 nm/min).

2.9. Rheology

Dynamic rheological measurements were performed on an AR2000 rheometer (TA Instruments) operating in oscillatory mode, equipped with a Peltier plate temperature control and a Couette geometry immersed inside the samples (300 µL), at 20 °C. Time sweep experiments were carried out at constant shearing stress (0.5%) and at a 1 rad/s angular frequency, followed by frequency (at a constant oscillatory stress of 1 Pa) and stress (at a constant angular frequency of 1 rad/s) sweep experiments.

2.10. Photothermal and drug release tests

The hydrogels were irradiated by the NIR laser (808 nm) at different powers (1, 2, or 4 W/cm^2) for 10 min (laser-sample distance: 3 cm). The temperature of the hydrogels was recorded in real time every minute for 10 min using the thermal imaging camera. After 10 min, the solution released from the hydrogel was removed and centrifuged (15000 g) at room temperature for 10 min.

Finally, the supernatant was collected and diluted 20 times to assess the amount of baclofen using HPLC (t_r = 7.2 min at λ = 220 nm).

2.11. Stability studies

After hydrogel formation (1 mL), 200 µL of 0.9% NaCl solution, RPMI and DMEM medium with 10% fetal bovine serum were slowly added to the top of the hydrogel. After 24 h, the released solution was collected and the total volume of supernatant was measured after centrifugation (15000 g, 10 min, room temperature). HPLC was employed to determine the concentration of baclofen in the released solution.

2.12. Data analysis

Each of the above set of experiments was repeated at least three times. The data are presented as means and standard deviations. Statistical analysis was performed using SPSS Statistics 26.0 and GraphPad Prism 9. Statistical variability between samples was shown as $*p < 0.05$, $**p < 0.01$, and $***p < 0.001$.

3. Results and discussion

3.1. Double network hydrogel formation

The preparation of the DN hydrogels is illustrated in **Figure 1**. Firstly, gel 1 and gel 2 (amino acid ratio of 1:1) were prepared based on our previous work (**Figure 1A**) [38]. Each amino acid (Fmoc-Tyr-OH, Fmoc-Tyr(Bzl)-OH, Fmoc-Phe-OH) was dissolved in DMSO to reach an initial concentration of 247 mM. 20 µL of a binary mixture (Fmoc-Tyr-OH/Fmoc-Tyr(Bzl)-OH (gel 1) or Fmoc-Phe-OH/Fmoc-Tyr(Bzl)-OH) (gel 2) were mixed with 1 mL of MilliQ® water to reach a final concentration of 4.9 mM in 2% DMSO/H_2O (v/v) solution. In parallel, APS and TEMED

were added into the acrylamide/bis-acrylamide or *N*-isopropylacrylamide/triethylene glycol dimethacrylate solutions to induce the free radical polymerization reaction to obtain PAAm or PNIPAAm (**Figure 1B**). Alternatively, an aqueous solution of agarose or L-agarose was heated at 90 °C for 10 min and left to cool down to room temperature (**Figure 1C**). Finally, a mixture of the photothermal agent and baclofen in water were added to the solution of the binary mixture of amino acids, followed by the addition of synthetic polymer or agarose/L-agarose solution (**Figure 1D**). In summary, to improve the properties of the amino-acid-based hydrogels, we introduced two different types of compounds (agarose/L-agarose and PAAm/PNIPAAm) able to self-assemble through different modes of interactions: while agarose/L-agarose gel formation is mainly driven by hydrogen bonds, PAAm/PNIPAAm is formed by covalent crosslinking.

To prepare such multicomponent hydrogels, we separately formulated both the amino acid (gel 1 or gel 2) and the agarose/L-agarose or PAAm/PNIPAAm solutions, considered as the primary and secondary networks, respectively. Then, the mixing of the two solutions led to the formation of a DN hydrogel, likely due to hydrogen bonding between the amino acids and PAAm/PNIPAAm or agarose/L-agarose. It is worth noting that all the gels exhibit a remarkable stability after mixing, and all components, especially the photothermal agents, are uniformly dispersed within the gel (**Figure 1**). As shown in **Figure S1A-B**, we observed that gel formation of gel 1 and gel 2 took around 1.5 h and 2 h, respectively, which could limit their application in the biomedical field. To obtain fast-forming amino-acid-based DN hydrogels with improved mechanical properties, we first optimized the concentration of the polymer. We observed that hydrogels with 5 or 10% PAAm or PNIPAAm (**Figure S2**) were stable, as well as 0.2, 0.5, or 1% agarose or

L-agarose hydrogels (**Figure S3**). In contrast, 1% PAAm or PNIPAAm formulation formed a solution, while the 0.1% agarose or L-agarose formulation led to a weak hydrogel (**Figure S2** and **Figure S3**). Remarkably, these formulations formed stable hydrogels when added into the amino acid solutions (**Figure S1C-J**). Therefore, the concentration of 1% PAAm/PNIPAAm and 0.1% agarose/L-agarose in the DN hydrogels was used for the rest of the study. The gelation times of 1% PAAm-gel 1, 1% PAAm-gel 2, 1% PNIPAAm-gel 1, and 1% PNIPAAm-gel 2 were between 15 and 30 min (**Figure S1C-F**). This result showed that PAAm or PNIPAAm rapidly formed DN hydrogels with the amino acid fibrils, thus accelerating the gelation process. In contrast, the addition of agarose or L-agarose did not affect the gelation time of gel 1 and gel 2 (**Figure S1G-J**). This might be because both agarose and amino acid hydrogels are stabilized by noncovalent interactions which are relatively weaker in nature.

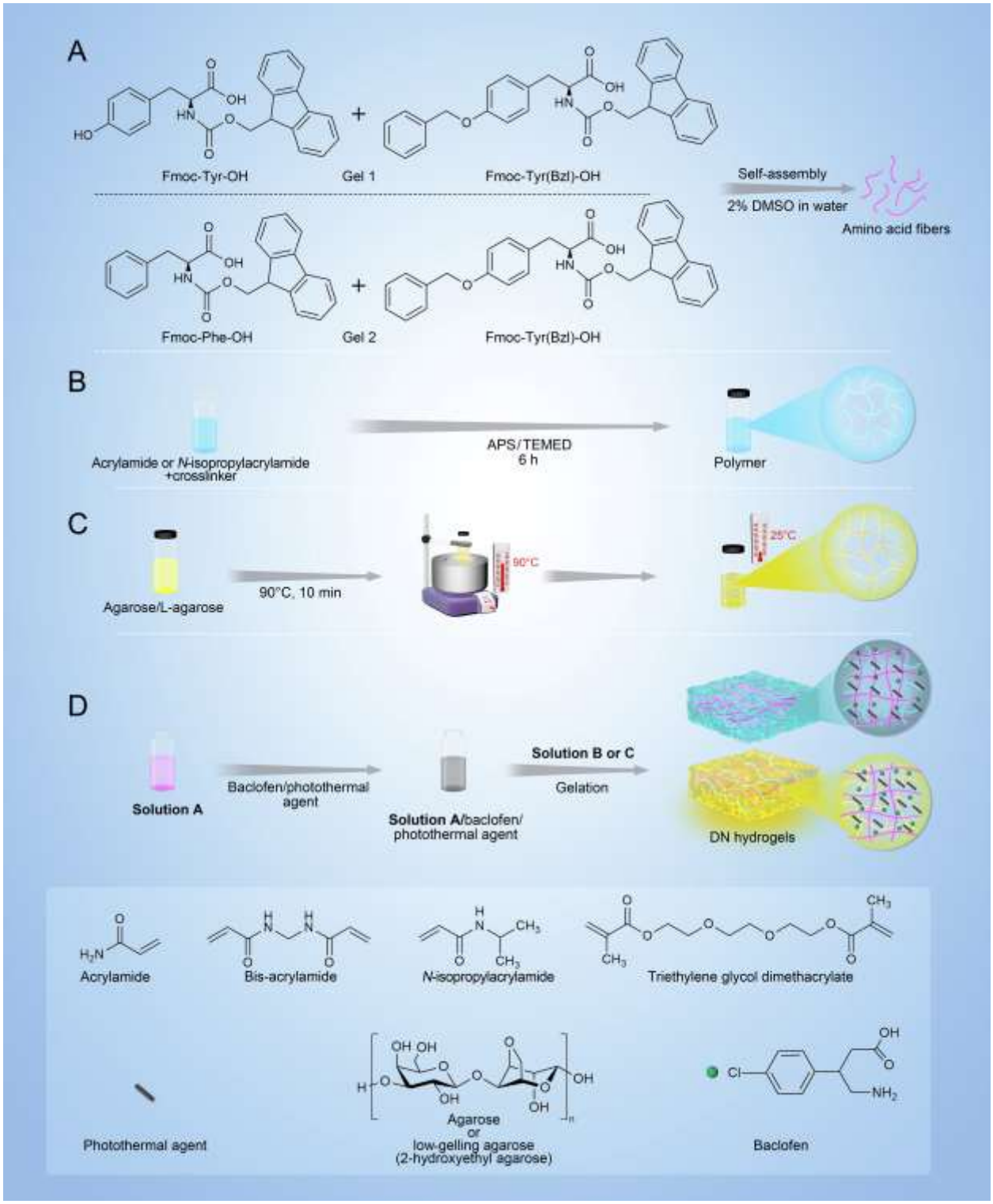

Figure 1. Schematic illustration of the formation of the solutions of amino acids (A), PAAm/PNIPAAm (B), and agarose/ L-agarose (C), and the DN hydrogels containing baclofen and the photothermal agents (D).

3.2. Optimization to minimize the residual monomer amounts

The residual amount of acrylamide or *N*-isopropylacrylamide monomer might induce some toxicity, as they are known neurotoxins [72,73]. Therefore, we used HPLC to quantify the amount of residual monomer in 1% PAAm or 1% PNIPAAm solutions after free-radical polymerization using different concentrations of APS and TEMED. The results showed that the remaining amount of monomer in 1% PAAm and 1% PNIPAAm solutions decreased with increasing volumes of APS and TEMED (**Figure 2A and 2B, Figure S4-S6**). The mixture of 200 μL of APS and 20 μL of TEMED were the conditions we used in the rest of the study. We verified that the polymers produced using these amounts of APS and TEMED could form stable DN hydrogels with gel 1 and gel 2 (**Figure S7**). Furthermore, to confirm the formation of the polymers used in the DN hydrogels, we characterized the hydrogels, monomers, and polymers formed in the absence of gel 1 or gel 2 by NMR and FTIR spectroscopies. The FTIR spectra showed that the intensity of the C=C vibration band in PAAm and PNIPAAm located at 1608 cm^{-1} and 1634 cm^{-1}, respectively, was significantly decreased compared to the monomers, as a result of the free-radical polymerization reaction (**Figure 2C and D**). In the ^{1}H NMR spectra, we observed the characteristic peaks of PAAm and PNIPAAm for the methylene protons (around 1.5 ppm) and methine protons (around 2.0 ppm) (**Figure 2E and F**) [74]. We also noticed that the NMR peak ratio of polymer to residual monomer in the DN hydrogels was 6:1 (1% PAAm-amino acid gel, **Figure S8**) and 9:1 (1% PNIPAAm-amino acid gel, **Figure S9**), respectively. These results fully confirmed the presence of polymers in the DN hydrogels.

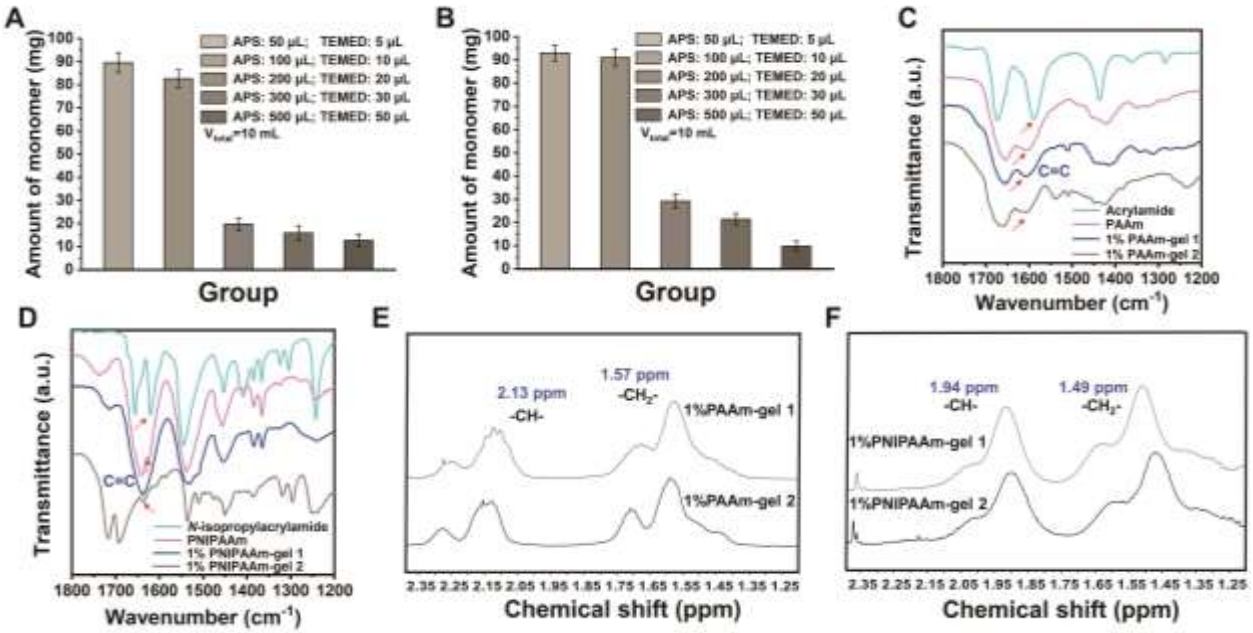

Figure 2. Residual amount of acrylamide (A) and *N*-isopropylacrylamide (B) monomer using different concentrations of APS and TEMED (the initial amount of monomer is 100 mg). Vertical bars indicate standard deviations (n=3). FTIR spectra of 1% acrylamide, 1% PAAm, 1% PAAm-gel 1 and 1% PAAm-gel 2 (C), and 1% *N*-isopropylacrylamide, 1% PNIPAAm, 1% PNIPAAm-gel 1 and 1% PNIPAAm-gel 2, (D); the red arrow shows the location of the C=C vibration band. ^{1}H NMR spectra of 1% PAAm-gel 1 and 1% PAAm-gel 2 (E), and 1% PNIPAAm-gel 1 and 1% PNIPAAm-gel 2 (F).

3.3. Optimization of the gelation times

A short gelation time is crucial for various biomedical applications [75-77]. Especially for the injectable gels, the gelation time must ideally be quick (usually within a few min), given that long gelation times may lead to the loss of injected solution in the body [78,79]. Therefore, another focus of this study was to shorten the gelation time by modulating the amino acid ratio. As shown in **Figure S10** and **Figure S11A-B**, after adjusting the ratio of Fmoc-Tyr-OH/Fmoc-Tyr(Bzl)-OH

(gel 1) or Fmoc-Phe-OH/Fmoc-Tyr(Bzl)-OH (gel 2) to 1:1.5 and 1:2, the gelation time of gel 1 and gel 2 was notably shortened compared with the 1:1 ratio. The gelation time of the amino acids was correlated to their concentration, probably because of faster self-assembly at higher concentrations [80]. Similarly, the gelation time of the DN hydrogels was significantly shortened by changing the ratio of amino acids from 1:1 to 1:1.5 and 1:2, probably because the higher amino acid concentration increased the density of the amino acid fibrils in the polymer network, favoring gelation (**Figure S11-13**). Indeed, the gelation time of 1% PAAm-gel 1, 1% PAAm-gel 2, 1% PNIPAAm-gel 1 and 1% PNIPAAm-gel 2 was less than 3 min, and in some cases, the gelation was nearly instantaneous (around 20 s) (**Figure S11C-D** and **Figure S12**). Similarly, the gelation time of 0.1% agarose-gel 1, 0.1% agarose-gel 2, 0.1% L-agarose-gel 1, and 0.1% L-agarose-gel 2 decreased to less than 50 min (**Figure S11E-F** and **Figure S13**). We then studied the incorporation of a photothermal agent in the DN hydrogels. Not only carbon-based nanomaterials (*e.g.*, GO, CNTs) are efficient photothermal agents, but also ICG and MoS_2 nanosheets [81,82]. The presence of a photothermal agent did not alter the gelation capacity of the different formulations (**Figure S14**). Nevertheless, we observed that the DN hydrogels loaded with the photothermal agent using an amino acid ratio of 1:2 were unable to release a high amount of water upon NIR light irradiation (808 nm, 2 W/cm^2, 10 min), contrary to the amino acid ratio 1:1.5 (**Figure S15**). Therefore, we decided to choose a ratio of 1:1.5 for the subsequent experiments. Additionally, we attempted to scale up the preparation of the DN hydrogels from 1 mL to 10 mL, and we again obtained stable hydrogels (**Figure S16**). These results indicate the optimizable character of the developed hydrogel system, which make it promising for wider applications.

3.4. Circular dichroism and transmission electron microscopy

To confirm whether the addition of the polymer affected the amino acid self-assembly process or not, we characterized the amino-acid-based and DN hydrogels using CD and TEM. All hydrogels had no CD signal at the initial time (t_0). After 1 h, however, gel 1 exhibited a negative band at ~220 nm, which was attributed to the π-π* phenyl side chain transition and hydrogen-bond network involving the carbamate functionality, and a weak broad positive band with a low intensity between 270 and 310 nm assigned to the n-π* Fmoc-Fmoc transition (**Figure 3A and 3C**) [38]. Two negative bands were observed for gel 2 around 220 nm and between 270 and 310 nm (**Figure 3B and 3D**). Most importantly, the DN hydrogels exhibited the same CD signals of gel 1 and gel 2 after 1 h, showing that the addition of the polymers, agarose, or L-agarose did not affect the self-assembly of the amino acids. TEM images showed that gel 1 is composed of a large number of fibrils with a diameter of 70 ± 14 nm (**Figure 3E-F**, **Figure S17A**). In the case of gel 2, the fibrils showed a slightly bigger width (108 ± 23 nm) compared to gel 1 (**Figure S17B**), but they were longer (**Figure 3G-H**). When gel 1 and gel 2 were mixed with the polymers, similar fibrils were observed (**Figure 3I-P**). However, the fibril width of 1% PAAm-gel 1, 1% PNIPAAm-gel 1, 1% PAAm-gel 2, and 1% PNIPAAm-gel 2 increased to 150 ± 21 nm, 205 ± 45 nm, 176 ± 32 nm, and 192 ± 45 nm, respectively (**Figure 3I-L, Figure S18A-B, E-F**). In 0.1% agarose-gel 1 (79 ± 16 nm), 0.1% L-agarose-gel 1 (88 ± 27 nm), 0.1% agarose-gel 2 (97 ± 11 nm), and 0.1% L-agarose-gel 2 (106 ± 22 nm), the fibrils had a similar width to that of the amino acid fibrils (**Figure 3M-P, Figure S18C-D, G-H**). Overall, the TEM images revealed that the polymers did not disrupt the amino acid self-assembly and could build DN hydrogels with the amino acid fibrils.

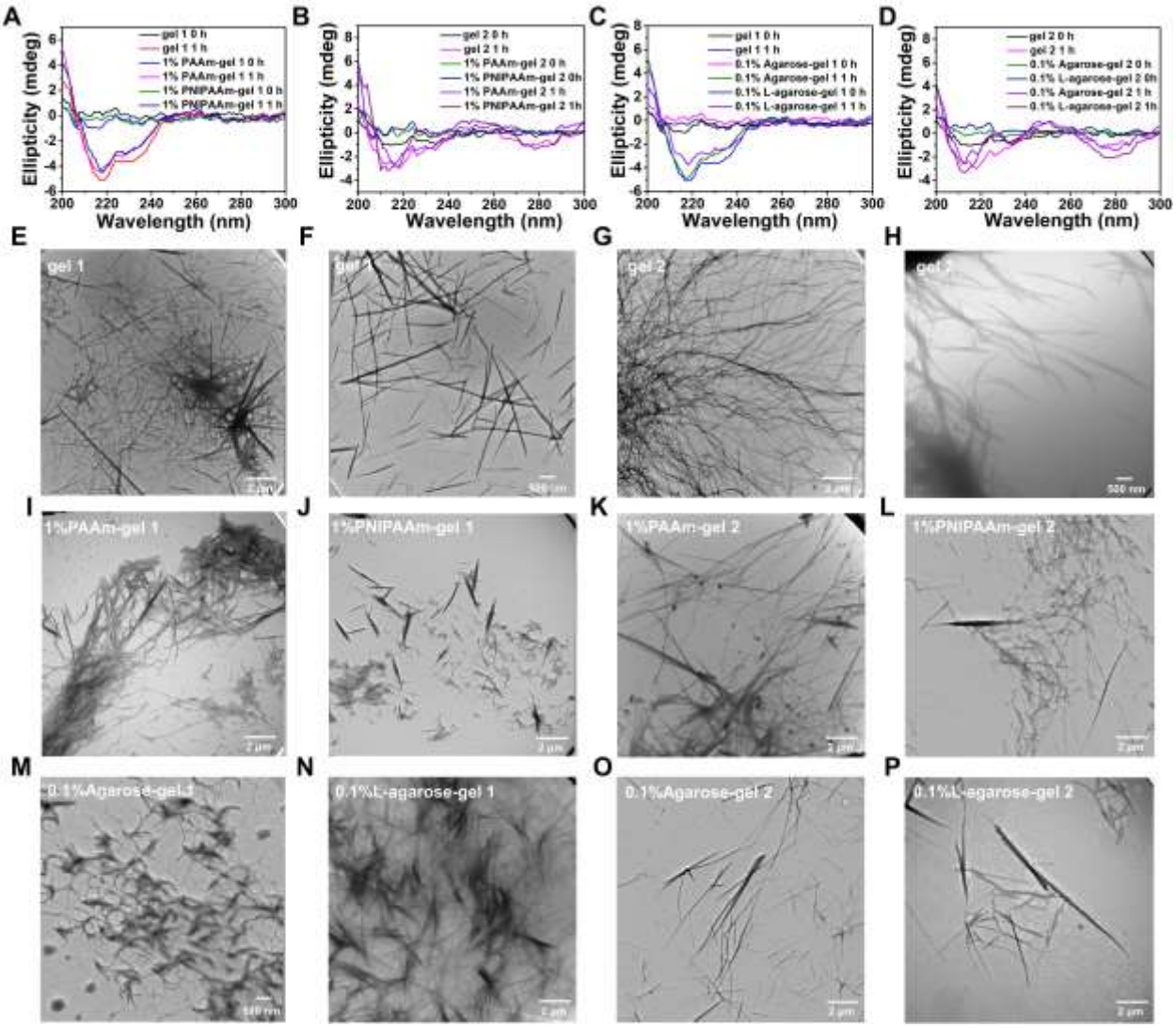

Figure 3. CD spectra of 1% PAAm-gel 1 and 1% PNIPAAm-gel 1 (A), 1% PAAm-gel 2 and 1% PNIPAAm-gel 2 (B), 0.1% agarose-gel 1 and 0.1% L-agarose-gel 1 (C), and 0.1% agarose-gel 2 and 0.1% L-agarose-gel 2 (D) at different time points; TEM images of gel 1 (E,F) and gel 2 (G,H), and 1% PAAm-gel 1 (I), 1% PNIPAAm-gel 1 (J), 1% PAAm-gel 2 (K), 1% PNIPAAm-gel 2 (L), 0.1% agarose-gel 1 (M), 0.1% L-agarose-gel 1 (N), 0.1% agarose-gel 2 (O), and 0.1% L-agarose-gel 2 (P).

3.5. Impact of the photothermal agents on the gelation time

The gelation time was similar or shorter when the hydrogels were loaded with the CNTs, GO, or MoS_2 nanosheets (**Figure S19**). In the case of ICG loading, the gelation time was similar or higher. The decrease of the gelation time when nanomaterials were incorporated in the hydrogels was certainly related to the high surface area of the nanomaterials that could promote the nucleation of the fibrils. To verify whether the optimized DN hydrogels could be used as injectable gels, we measured the gelation time at human body temperature. The gelation time of all the DN hydrogels formed at the 1:1.5 amino acid ratio was significantly reduced at 37 °C compared with the 1:1 ratio (**Figure 4** and **Figure S20**). Moreover, the gelation time of 1% PAAm-gel 1, 1% PNIPAAm-gel 1, 1% PAAm-gel 2 and 1% PNIPAAm-gel 2 loaded with the photothermal agents was less than 10 min, which is relevant for their application as injectable hydrogels. However, the gelation time of 0.1% agarose-gel 1, 0.1% L-agarose-gel 1, 0.1% agarose-gel 2 and 0.1% L-agarose-gel 2 exceeded 60 min. This may be related to the gelation critical temperature of agarose and L-agarose being lower than 37 °C [83,84]. For all hydrogels, the gelation time at 37 °C was notably higher than that of at room temperature.

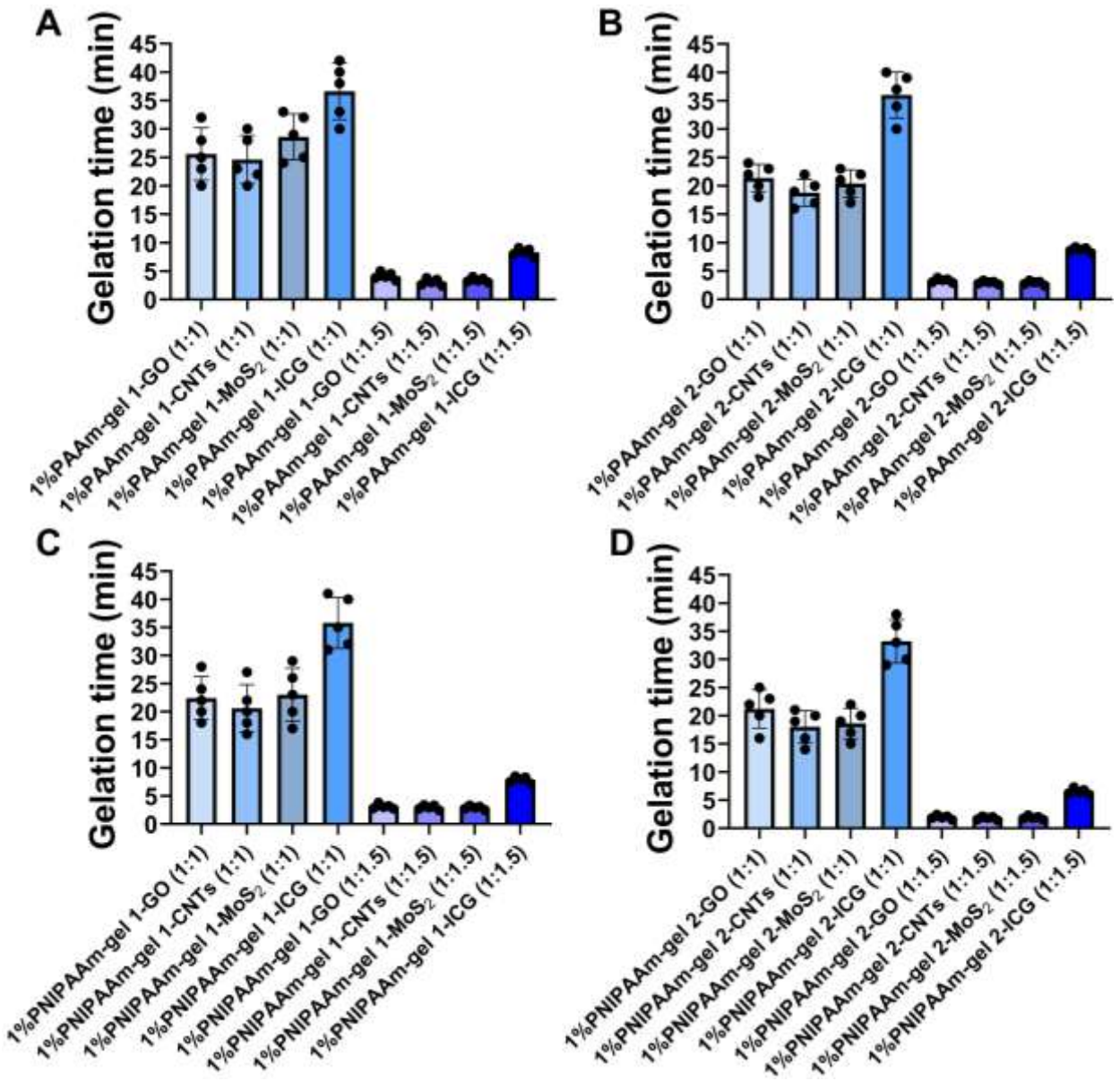

Figure 4. Gelation time of the DN hydrogels loaded with the four photothermal agents at 37 ℃ when different amino acids are used at different ratios: 1% PAAm-gel 1 (A), 1% PAAm-gel 2 (B), 1% PNIPAAm-gel 1 (C), and 1% PNIPAAm-gel 2 (D). The ratio of Fmoc-Tyr-OH/Fmoc-Tyr(Bzl)-OH or Fmoc-Phe-OH/Fmoc-Tyr(Bzl)-OH was 1:1 (2.45:2.45 mM) or 1:1.5 (2.45:3.75 mM). Each solid circle indicates a single measurement, and the vertical bars indicate standard

deviations (n=5). Note that, irrespective of the gel system and photothermal agent used, we observed a clear transition (drop) in gelation times when the amino acid ratio was 1:1.5 instead of 1:1.

3.6. Photothermal and drug release study

We decided to load baclofen, a model drug used for treating severe spasticity [85], into the DN hydrogels at a concentration of 0.96 mg/mL. We investigated the efficiency of the different photothermal agents in triggering the drug release under NIR light irradiation. We first evaluated the photothermal capacity of the four photothermal agents dispersed in water under irradiation at 808 nm and using different laser powers for 10 min (**Figure S21**). A higher temperature increase was observed for ICG and CNTs compared to GO and MoS_2 nanosheets. The same tendency was found for the DN hydrogels loaded with the photothermal agents independently of the laser power (**Figure 5**, **Figure S22**, and **Figure S23**). The temperature increased more for higher laser powers and was not dependent on the type of DN hydrogels, whatever they were composed of covalent bonds (PAAm/PNIPAAm) or noncovalent bonds (agarose/L-agarose).

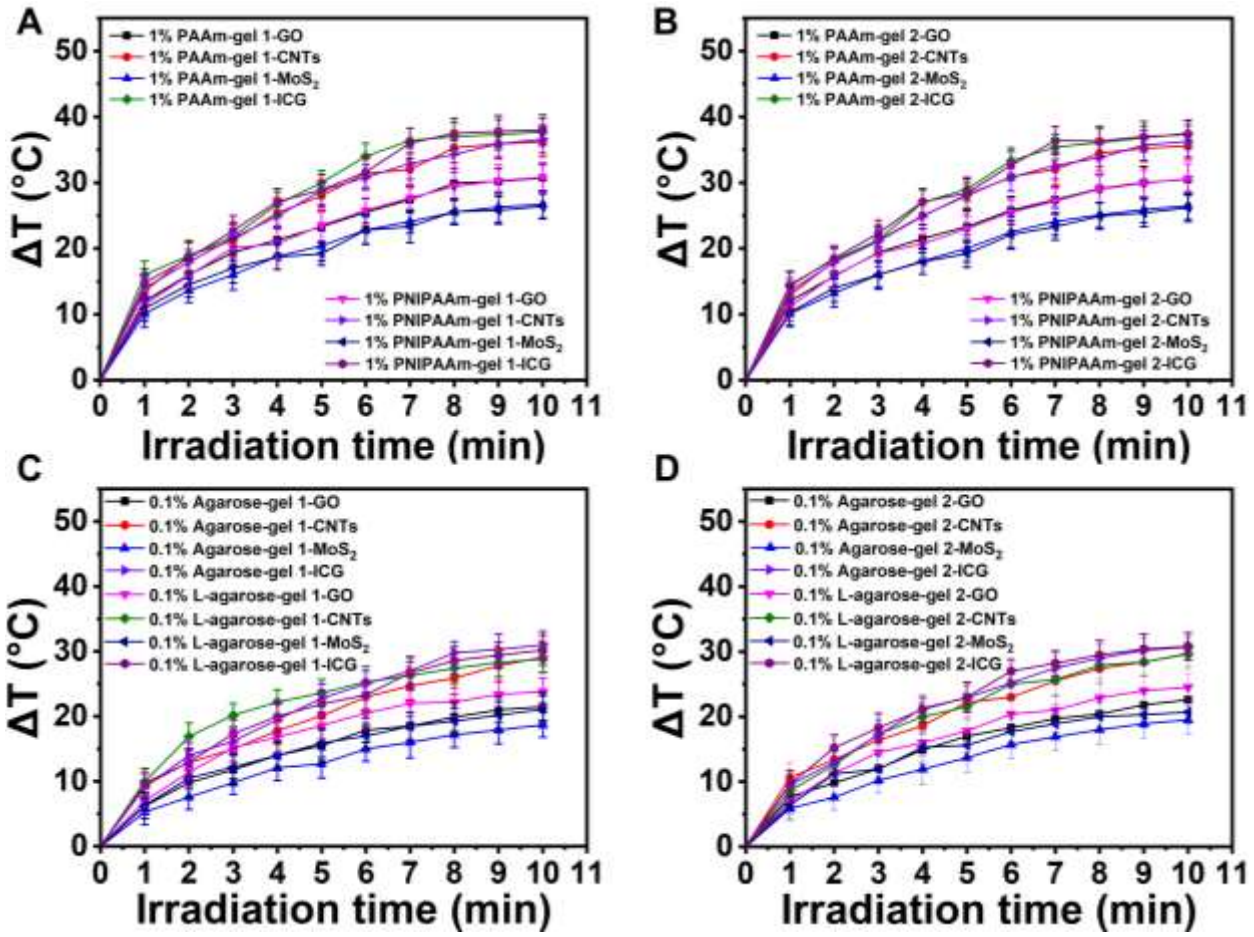

Figure 5. Temperature increase of 1% PAAm (or 1% PNIPAAm)-gel 1 loaded with the four photothermal agents (A), 1% PAAm (or 1% PNIPAAm)-gel 2 loaded with the four photothermal agents (B), 0.1% agarose (0.1% L-agarose)-gel 1 loaded with the four photothermal agents (C) and 0.1% agarose (0.1% L-agarose)-gel 2 loaded with the four photothermal agents (D) when exposed to a NIR laser (at 808 nm, 2 W/cm^2). The vertical bars indicate standard deviations (n=3).

After treating the different DN hydrogels loaded with baclofen and a photothermal agent with NIR light for 10 min, we collected the water released from the hydrogels, quantified its volume, and assessed the amount of baclofen by HPLC using a calibration curve (**Figure S24**). We observed that the amount of released water and baclofen was correlated with the laser power for all the DN hydrogels (**Figure 6** and **Figure S25-28**). Indeed, the release of water was the lowest at 1

W/cm^2 (agarose- and L-agarose-based DN hydrogels were stable in these conditions and there was no water/drug release), and it was the highest at 4 W/cm^2. As shown in **Figure S26**, the water release rate of PAAm/PNIPAAm-based DN hydrogels was in the range of 50-65% under NIR light irradiation at 2 W/cm^2, but it was lower for agarose/L-agarose-based DN hydrogels (30-65%). This difference was probably caused by the fact that agarose and L-agarose in the DN hydrogels did not reach a complete gel-to-sol transition state under this low-power irradiation [83]. However, it is worth noting that the water release rate of the 0.1% L-agarose-DN hydrogels was higher than that of the 0.1% agarose DN hydrogels in these conditions (**Figure S26C-D**). This is likely because L-agarose has a lower gel-to-sol transition temperature than agarose [49]. All agarose- and L-agarose-based DN hydrogels showed a higher release of water when loaded with ICG and CNTs **(Figure S25A-B**, **Figure S26**, and **Figure S27**), independently of the laser power, indicating that the water released from these hydrogels was related to the photothermal behavior of the hydrogels, as ICG and CNTs showed better photothermal performance than GO and MoS_2 nanosheets (**Figure 5**). We noted that the release of baclofen from the DN hydrogels correlated well with the release of water. The baclofen release from the PAAm/PNIPAAm-based DN hydrogels was in the range of 40-60%, whereas it was between 25 and 60% from the agarose/L-agarose-based DN hydrogels at a laser power of 2 W/cm^2 (**Figure 6**). Interestingly, we observed less difference between the PAAm/PNIPAAm- or agarose/L-agarose-based hydrogels at 4 W/cm^2, showing a drug release of ~55-80% (**Figure S28**). In all cases, the MoS_2-loaded hydrogels showed the lowest drug release rate.

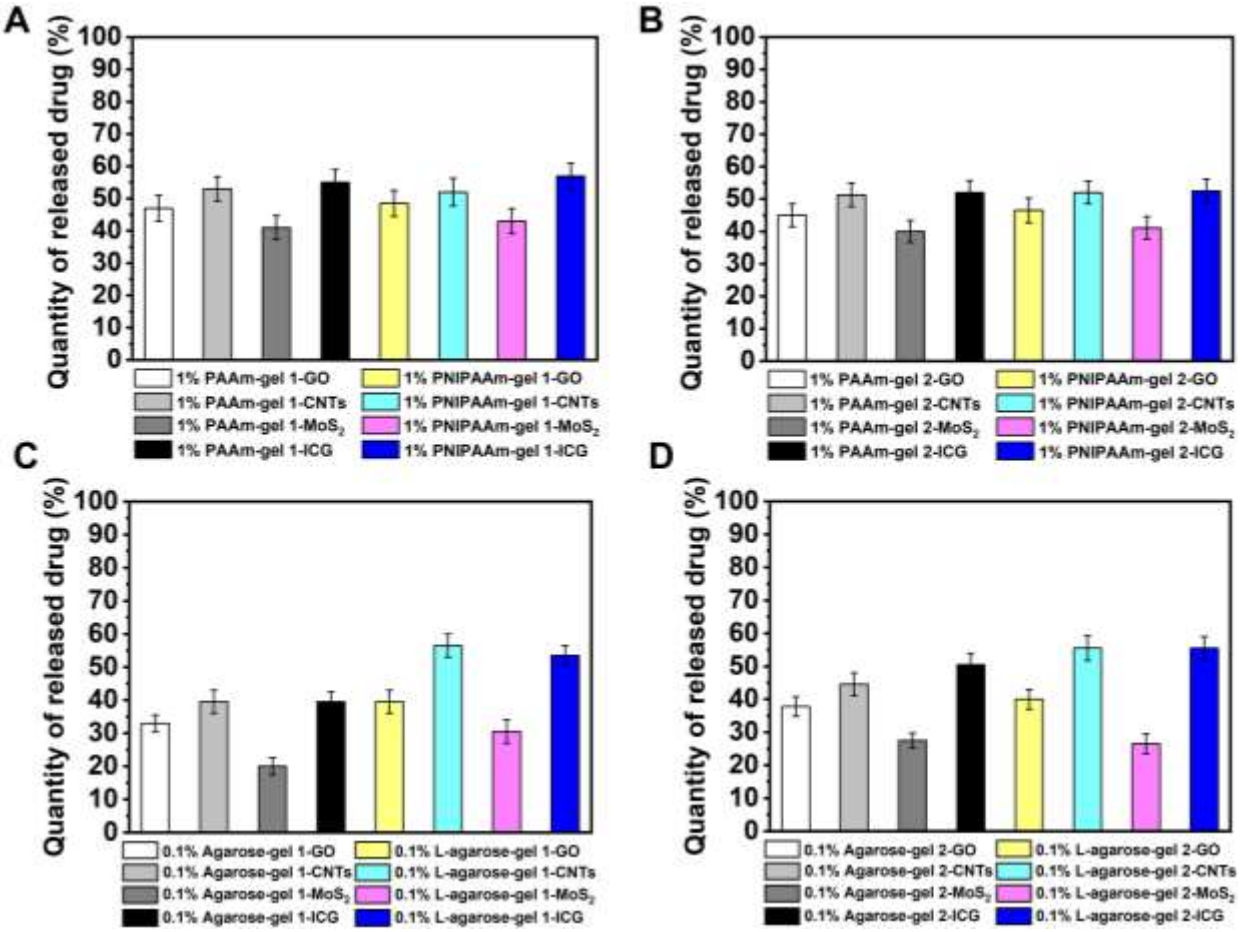

Figure 6. Drug release from 1% PAAm (or 1% PNIPAAm)-gel 1 loaded with the four photothermal agents (A), 1% PAAm (or 1% PNIPAAm)-gel 2 loaded with the four photothermal agents (B), 0.1% agarose (0.1% L-agarose)-gel 1 loaded with the four photothermal agents (C), and 0.1% agarose (0.1% L-agarose)-gel 2 loaded with the four photothermal agents (D) when exposed to a NIR laser (at 808 nm, 2 W/cm^2). The vertical bars indicate standard deviations (n=3).

We can conclude that the CNTs were the best photothermal agents to incorporate in our hydrogels because of their high photothermal conversion efficiency for a low power density (808 nm, 1-2 W/cm^2) [86-89]. Such laser power density does not lead to bystander tissue damage [90-93]. In addition, the drug release from the CNT-loaded hydrogels was generally higher compared to the GO-loaded hydrogels. In contrast, the hydrogels loaded with the MoS_2 nanosheets showed

the lowest drug release, while the gelation time of the ICG-loaded DN hydrogels was higher compared to the other photothermal agents. Nevertheless, the drug release capacity of the DN hydrogels was similar (up to ~80%) at the highest laser power, showing that the type of amino acids and polymers did not alter the performance of the hydrogels at beyond a certain threshold.

3.7. Rheological and stability study

Finally, to assess the impact of the presence of a secondary network (*e.g.*, PAAm or agarose) on the mechanical properties of amino-acid-based hydrogels, we carried out rheological experiments using the CNT-loaded formulations. Frequency sweep data of the samples (**Figure 7A**) exhibited characteristic viscoelastic solid behaviors (with storage moduli G' > loss moduli G"), confirming the formation of a hydrogel for gel 2-CNTs-baclofen, which was also the case with 1% PAAm or 0.1% agarose. However, while the presence of agarose did not impact the mechanical properties of gel 2-CNTs-baclofen (G' ~ 100 Pa, G" ~ 20 Pa), PAAm markedly improved the stiffness of the gel, with G' > 1000 Pa. Such differences can be explained by the inherent chemical structure of the added compounds, with agarose mainly interacting *via* noncovalent bonds (such as hydrogen bonds), whereas the PAAm network is held together by covalent bonds. To follow the gelation process, time sweep experiments were performed (**Figure 7B-D**). Interestingly, at the beginning of the measurement (*i.e.*, a few tens of seconds after the formulation), all samples were in a gel state (G' > G") even if weak, showing that very fast gelation processes occurred, with or without the presence of a DN. However, a short period of time was necessary to reach a plateau and to macroscopically observe the sol-to-gel transition, which was the fastest for the 1% PAAm-gel 2-CNTs-baclofen sample (3 min) compared to the 0.1% agarose-gel 2-CNTs-baclofen and gel

2-CNTs-baclofen hydrogels, with a sol-to-gel transition time of 15 and 13 min, respectively. Once more, these data highlight that the DN formed with PAAm induced a significant improvement of the mechanical (with stiffness improved by a factor of ~10 times) and kinetics (4 times faster) properties of the hydrogels, confirming their interest. A storage modulus (G') value of ~1 kPa is sufficient to design injectable hydrogels that are stable in the organism [94,95]. The lower mechanical strength of agarose-based DN hydrogels in comparison to the PAAm-based DN hydrogels probably stems from the weak hydrogen bonds driving the agarose gel formation compared to the covalent crosslinking of the acrylamide monomers leading to PAAm.

Besides, carbon-based nanomaterials and MoS_2 have been frequently employed as reinforcement agents in hydrogels owing to their remarkable mechanical strength. In this case, a rather high content of such materials is needed, for example in the range 0.08-5.00 wt% [96-102]. In contrast, we loaded our hydrogels with a much smaller amount of CNTs, GO, MoS_2, and ICG (only 0.0125 wt%). In our previous work, we conducted a comparative study of the mechanical properties of the amino-acid-based hydrogels (gel 1 and gel 2) and the hydrogels loaded with carbon nanomaterials (gel 1 and gel 2 loaded with 0.025 wt% CNTs or GO). Those explorations revealed that gel 1 and gel 2 exhibited a similar modulus of rigidity, and the addition of 0.025 wt% CNT or GO had no notable impact on the mechanical strength of either gel 1 or gel 2 [38]. However, this concentration is sufficient to induce a photothermal effect to satisfy our drug release requirements.

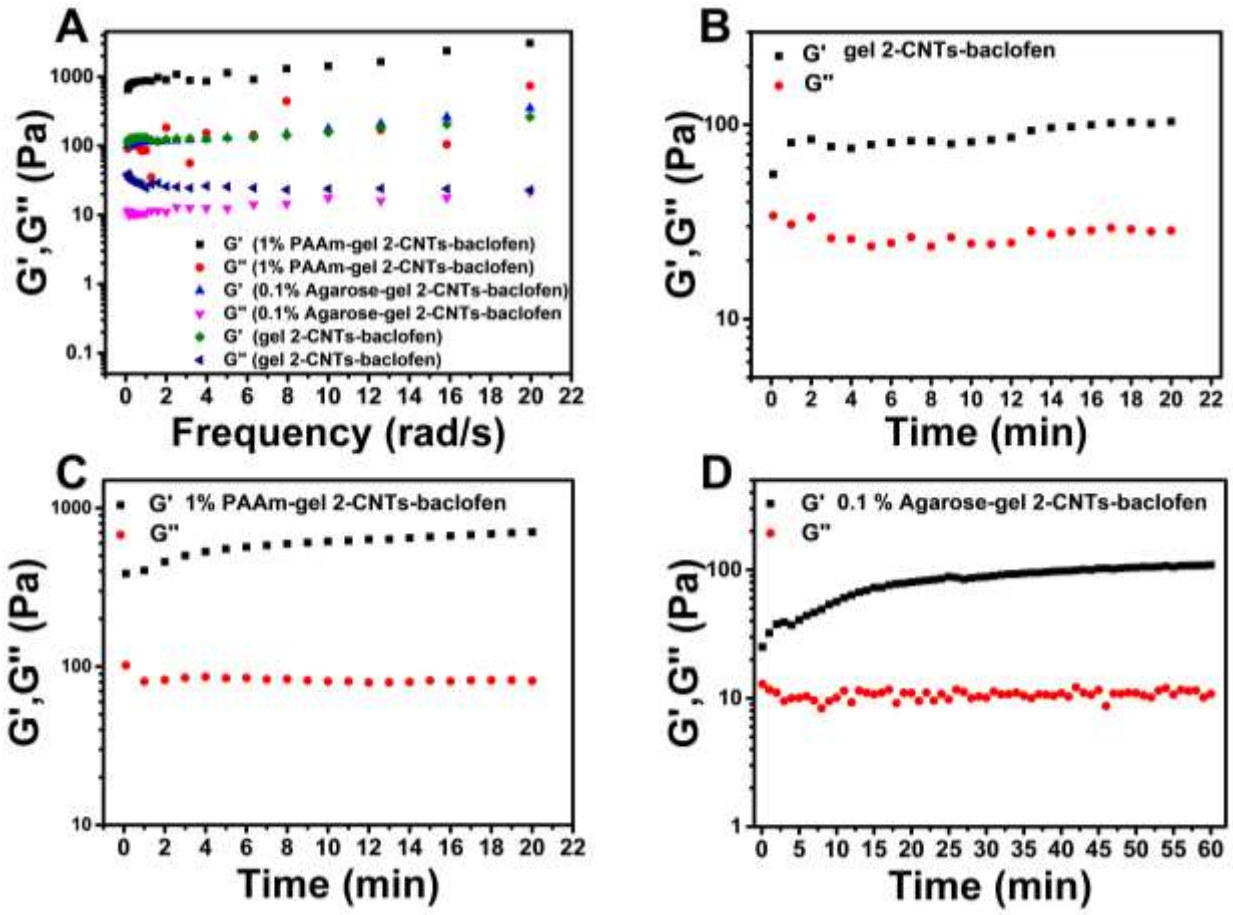

Figure 7. Frequency sweep of gel 2-CNTs-baclofen, 1% PAAm-gel 2-CNTs-baclofen, 0.1% agarose-gel 2-CNTs-baclofen at 20 °C (A). Evolution of the storage modulus (G') and loss modulus (G'') as a function of time for gel 2-CNTs-baclofen (B), 1% PAAm-gel 2-CNTs-baclofen (C), and 0.1% agarose-gel 2-CNTs-baclofen (D).

The stability of the DN hydrogels in physiological environments (0.9% NaCl solution, RPMI or DMEM medium) was studied (**Figure S29-31**). After 24 h, all hydrogels showed a water and drug release below 15% in the three physiological environments, suggesting good stability. In comparison, the water release from the gel 2-based DN hydrogels was lower than that of the gel 1-based DN hydrogels in some cases. We observed no major difference of stability between the PAAm/PNIPAAm-based DN hydrogels and between the agarose/L-agarose-based-DN hydrogels.

Taken together, we have successfully designed stable DN hydrogels using amino acids and polymers or agarose/L-agarose. The addition of a photothermal agent endows the DN hydrogels with NIR-responsiveness and photothermal behavior. The DN hydrogels can carry high doses of baclofen and release large amounts of the drug under NIR light irradiation. The water and drug release rates can be adjusted with the power of NIR light. Our strategy has allowed us to overcome the low mechanical strength and long gelation time of amino-acid-based hydrogels. The high mechanical properties of the hydrogels, rapid gel formation, and adjustable drug release properties under NIR light irradiation could enable their use as subcutaneous injectable hydrogels, which would represent an alternative to the continuous intrathecal pumps for controlled release of baclofen *in vivo* and spasticity treatment. There is a limited number of studies in the literature on the design of hydrogels for the controlled release of baclofen through an oral or intrathecal administration [4,5,103]. Although these previously reported hydrogels are able to achieve cumulative baclofen release rates of over 80% in a sustained-release process of several hours, they have some limitations. For example, the sustained-release process is generally difficult to control, especially during the initial stage of the drug release. This can be problematic, as a large release of baclofen can lead to toxic effects [4,103]. For instance, the instability of chitosan thermosensitive gels in the gelling process at body temperature makes the release of baclofen unpredictable [5]. Therefore, our NIR-responsive hydrogels are promising alternatives for the controlled baclofen release. Among all the different formulations we tested, we found that the PAAm/PNIPAAm-gel 2 hydrogels loaded with the oxidized CNTs and baclofen have the highest drug release capacity while

displaying high mechanical properties and good stability under physiological conditions. The innovative aspect of our work lies in the simplicity of the synthesis process, distinguishing it from most existing literature that often involves complex and tedious preparation steps [44].

4. Conclusion and outlook

In this study, our primary objective was to design photothermally responsive DN hydrogels for baclofen release. The first network, consisting of amino acids, is physically crosslinked, allowing for the incorporation of a second network that can be either physically or chemically crosslinked, resulting in the formation of physical/physical DN hydrogels or physical/chemical DN hydrogels. These two categories of DN hydrogels may exhibit variations in gelation time, mechanical properties, and drug release capacity. Agarose and PAAm are exemplary polymers that can be either physically or chemically crosslinked and are frequently employed as secondary networks within the gel, especially photothermal responsive hydrogels. Hence, agarose and PAAm were selected as subjects of comparison in this study, to explore the distinctions between physical/physical and physical/chemical DN hydrogels concerning essential aspects such as gelation kinetics, mechanical characteristics, and drug release behavior. This investigation sought to determine which type of DN hydrogel (physical/physical crosslinked or physical/chemical crosslinked) could find potential utility in our subsequent biological applications.

We have synthesized a series of stable amino acid/polymer-based (PAAm/PNIPAAm, agarose/L-agarose) DN hydrogels with a low gelation time, high drug loading, and NIR-responsive drug release capacity. We confirmed the formation of PAAm and PNIPAAm polymers by FTIR

and NMR spectroscopy. We optimized the formulation to decrease the residual amount of acrylamide or *N*-isopropylacrylamide monomers, thus minimizing the risk associated to their toxicity. The conditions were also tuned to shorten the gelation time and enhance the mechanical properties of the hydrogels. Adjusting the ratio of the amino acids (Fmoc-Tyr-OH/Fmoc-Tyr(Bzl)-OH or Fmoc-Phe-OH/Fmoc-Tyr(Bzl)-OH) significantly decreased the gelation time. At body temperature, the gelation time of the 1% PAAm- or 1% PNIPAAm-based DN hydrogels was less than 10 min. These hydrogels remained stable under physiological environment, meeting a key standard for injectable gels. All the DN hydrogels could carry a high load of baclofen and release a high dose of the drug under NIR light irradiation, providing perspectives for the controlled administration of baclofen. Besides, we demonstrated that the formation of polymers in the supramolecular amino acid fibril network enhanced the mechanical properties of the hydrogels in comparison to the addition of agarose.

In future work, we will assess the ability of the DN hydrogels for sustained release of baclofen *in vivo* and their therapeutic efficiency to treat severe spasticity. We will also expand our hydrogels to other types of drugs and evaluate their release profile, which will enormously broaden the biomedical application potential of our DN hydrogels. Secondly, the gelation time and mechanical strength of the agarose/L-agarose-based DN hydrogels are the areas that require further optimization to enhance their overall performance. Addressing these aspects would contribute to the improved efficacy and utility of our hydrogels. We also plan to evaluate the biocompatibility of the DN hydrogels. As an alternative to the intrathecal baclofen therapy using pumps, we also aim to inject our DN hydrogels subcutaneously *in vivo* in a spasticity mouse model, to precisely modulate

the release of baclofen in a spatiotemporally controlled and sustained manner. The liberation of baclofen would be remotely triggered upon NIR light irradiation, thus avoiding the implantation of an intrathecal minipump with possible adverse events.

CRediT authorship contribution statement

A.B. and C.M.-M. designed and supervised the work and revised the draft. S.X. performed most experiments, analyzed the data, and wrote the draft. C.G.-C. contributed to hydrogel synthesis and preliminary experiments. P.H. and L.S. performed the rheological study. All authors read and revised the manuscript.

Declaration of competing interest

The authors declare that they have no known competing financial interests or personal relationships that could have appeared to influence the work reported in this paper.

Acknowledgements

We wish to acknowledge the Centre National de la Recherche Scientifique (CNRS) and the International Center for Frontier Research in Chemistry (icFRC). The authors wish to thank Cathy Royer from the “Plateforme Imagerie In Vitro de l'ITI Neurostra,” CNRS UAR 3156, University of Strasbourg (Strasbourg, France) for TEM analyses. We gratefully acknowledge Rym Soltani, Céline Corcelle and Riccardo Pinotti for the preparation of the oxidized CNTs, and Yilin He for helping with the exfoliation of MoS_2. S. Xiang is indebted to the China Scholarship Council (CSC) for supporting his PhD. The authors also thank Dr. H. E. Karahan for providing critical feedback on the manuscript and editing.

References

[1] R.R. Young, Spasticity: a review, Neurology. 44 (11 Suppl 9) (1994) S12-20, http://intl.neurology.org/cgi/content/abstract/44/11

[2] P. Flachenecker, T. Henze, U.K. Zettl, Spasticity in patients with multiple sclerosis-clinical characteristics, treatment and quality of life, Acta Neurol. Scand. 129 (3) (2014) 154-162, https://doi.org/10.1111/ane.12202

[3] E. Ghasemian, A. Vatanara, N. Navidi, M.R. Rouini, Brain delivery of baclofen as a hydrophilic drug by nanolipid carriers: Characteristics and pharmacokinetics evaluation, J. Drug Delivery Sci. Technol. 37 (2017) 67-73, https://doi.org/10.1016/j.jddst.2016.06.012

[4] I.A. El-said, A.A. Aboelwafa, R.M. Khalil, O.N. ElGazayerly, Baclofen novel gastroretentive extended release gellan gum superporous hydrogel hybrid system: *in vitro* and *in vivo* evaluation, Drug Deliv. 23 (1) (2016) 101-112, https://doi.org/10.3109/10717544.2014.905654

[5] F. Lagarce, N. Faisant, J.C. Desfontis, L. Marescaux, F. Gautier, J. Richard, P. Menei, J.P. Benoit, Baclofen-loaded microspheres in gel suspensions for intrathecal drug delivery: *in vitro* and *in vivo* evaluation, Eur. J. Pharm. Biopharm. 61 (3) (2005) 171-180, https://doi.org/10.1016/j.ejpb.2005.04.004

[6] K. Nigam, A. Kaur, A. Tyagi, K. Manda, N. Goswami, M. Nematullah, F. Khan, R. Gabrani, P. Gauba, S. Dang, *In vitro* & *in vivo* evaluations of PLGA nanoparticle based combinatorial drug therapy for baclofen and lamotrigine for neuropathic pain management, J. Microencapsulation. 39 (2) (2022) 95-109, https://doi.org/10.1080/02652048.2022.2041751

[7] J. Li, D. J. Mooney. Designing hydrogels for controlled drug delivery. Nat. Rev. Mater. 1 (12) (2016) 1-17. https://doi.org/10.1038/natrevmats.2016.71

[8] R. Chakrabarty, P.S. Mukherjee, P.J. Stang, Supramolecular coordination: self-assembly of fi nite two- and three-dimensional ensembles, Chem. Rev. 111 (11) (2011) 6810-6918, https://doi.org/10.1021/cr200077m

[9] M.E. Carnes, M.S. Collins, D.W. Johnson, Transmetalation of self-assembled, supramolecular complexes, Chem. Soc. Rev. 43 (6) (2014) 1825-1834, https://doi.org/10.1039/C3CS60349K

[10] S. Fleming, R.V. Ulijn, Design of nanostructures based on aromatic peptide amphiphiles, Chem. Soc. Rev. 43 (23) (2014) 8150-8177, https://doi.org/10.1039/C4CS00247D

[11] D.K. Kumar, J.W. Steed, Supramolecular gel phase crystallization: orthogonal self-assembly under non-equilibrium conditions, Chem. Soc. Rev. 43 (7) (2014) 2080-2088, https://doi.org/10.1039/C3CS60224A

[12] P. Chakraborty, E. Gazit, Amino acid based self-assembled nanostructures: complex structures from remarkably simple building blocks, ChemNanoMat. 4 (8) (2018) 730-740, https://doi.org/10.1002/cnma.201800147

[13] C.B.P. Oliveira, V. Gomes, P.M.T. Ferreira, J.A. Martins, P.J. Jervis, Peptide-based supramolecular hydrogels as drug delivery agents: recent advances, Gels 8. (11) (2022) 706, https://doi.org/10.3390/gels8110706

[14] S.E. Paramonov, H.W. Jun, J.D. Hartgerink, Self-assembly of peptide-amphiphile nanofibers: the roles of hydrogen bonding and amphiphilic packing, J. Am. Chem. Soc. 128 (22) (2006) 7291-7298, https://doi.org/10.1021/ja060573x

[15] J. Kopeček, J. Yang, Peptide-directed self-assembly of hydrogels, Acta Biomater. 5 (3) (2009) 805-816, https://doi.org/10.1016/j.actbio.2008.10.001

[16] F. Raza, H. Zafar, X. You, A. Khan, J. Wu, L. Ge, Cancer nanomedicine: focus on recent de velopments and self-assembled peptide nanocarriers, J. Mater. Chem. B. 7 (48) (2019) 7639-765 5, https://doi.org/10.1039/C9TB01842E

[17] S. Xian, M.J. Webber, Temperature-responsive supramolecular hydrogels, J. Mater. Chem. B. 8 (40) (2020) 9197-9211, https://doi.org/10.1039/D0TB01814G

[18] G. Fichman, E. Gazit, Self-assembly of short peptides to form hydrogels: design of building blocks, physical properties and technological applications, Acta Biomater. 10 (4) (2014) 1671-16 82, https://doi.org/10.1016/j.actbio.2013.08.013

[19] M.J. Webber, E.T. Pashuck, (Macro)molecular self-assembly for hydrogel drug delivery, Ad v. Drug Deliv. Rev. 172 (2021) 275-295, https://doi.org/10.1016/j.addr.2021.01.006

[20] J. Zhang, W. Lin, L. Yang, A. Zhang, Y. Zhang, J. Liu, J. Liu, Injectable and pH-responsive self-assembled peptide hydrogel for promoted tumor cell uptake and enhanced cancer chemother apy, Biomater. Sci. 10 (3) (2022) 854-862, https://doi.org/10.1039/D1BM01788H

[21] D. Marin, S. Marchesan, Self-assembled peptide nanostructures for ECM biomimicry, Nano materials. 12 (13) (2022) 2147, https://doi.org/10.3390/nano12132147

[22] A. Mahler, M. Reches, M. Rechter, S. Cohen, E. Gazit, Rigid, Self-assembled hydrogel com posed of a modified aromatic dipeptide, Adv. Mater. 18 (11) (2006) 1365-1370, https://doi.org/1 0.1002/adma.200501765

[23] A.M. Smith, R.J. Williams, C. Tang, P. Coppo, R.F. Collins, M.L. Turner, A. Saiani, R.V. U lijn, Fmoc-diphenylalanine self assembles to a hydrogel via a novel architecture based on π-π inte rlocked β-sheets, Adv. Mater. 20 (1) (2008) 37-41, https://doi.org/10.1002/adma.200701221

[24] C. Gila-Vilchez, M.C. Mañas-Torres, Ó. D. García-García, A. Escribano-Huesca, L. Rodríguez-Arco, V. Carriel, L. Álvarez de Cienfuegos, Biocompatible short-peptides fibrin co-assembled hydrogels. ACS Appl. Polym. Mater. 5 (3) (2023) 2154-2165, https://doi.org/10.1021/acsapm.2c02164

[25] A.L. Rodriguez, T.Y. Wang, K.F. Bruggeman, C.C. Horgan, R. Li, R.J. Williams, D.R. Nisbet, *In vivo* assessment of grafted cortical neural progenitor cells and host response to functionalized self-assembling peptide hydrogels and the implications for tissue repair, J. Mater. Chem. B. 2 (44) (2014) 7771-7778, https://doi.org/10.1039/C4TB01391C

[26] K. Tao, A. Levin, L. Adler-Abramovich, E. Gazit, Fmoc-modified amino acids and short peptides: simple bio-inspired building blocks for the fabrication of functional materials, Chem. Soc. Rev. 45 (14) (2016) 3935-3953, https://doi.org/10.1039/C5CS00889A

[27] A. Baral, S. Roy, S. Ghosh, D. Hermida-Merino, I.W. Hamley, A. Banerjee, A Peptide-based mechano-sensitive, proteolytically stable hydrogel with remarkable antibacterial properties, Langmuir. 32 (7) (2016) 1836-1845, https://doi.org/10.1021/acs.langmuir.5b03789

[28] S. Eskandari, T. Guerin, I. Toth, R.J. Stephenson, Recent advances in self-assembled peptides: implications for targeted drug delivery and vaccine engineering, Adv. Drug Deliv. Rev. 110 (2017) 169-187, https://doi.org/10.1016/j.addr.2016.06.013

[29] P. Vlieghe, V. Lisowski, J. Martinez, M. Khrestchatisky, Synthetic therapeutic peptides: science and market, Drug Discovery Today. 15 (1-2) (2010) 40-56, https://doi.org/10.1016/j.drudis.2009.10.009

[30] S. Wang, X. Liu, I.J. Villar-Garcia, R. Chen, Amino acid based hydrogels with dual responsiveness for oral drug delivery, Macromol Biosci. 16 (9) (2016) 1258-1264, https://doi.org/10.1002/mabi.201600078

[31] Q. Zhao, Y. Zhao, Z. Lu, Y. Tang, Amino acid-modified conjugated oligomer self-assembly hydrogel for efficient capture and specific killing of antibiotic-resistant bacteria, ACS Appl. Mater. Interfaces. 11 (18) (2019) 16320-16327, https://doi.org/10.1021/acsami.9b02643

[32] I. Irwansyah, Y.Q. Li, W. Shi, D. Qi, W.R. Leow, M.B.Y. Tang, S. Li, X. Chen, Gram-positive antimicrobial activity of amino acid-based hydrogels, Adv. Mater. 27 (4) (2015) 648-654, https://doi.org/10.1002/adma.201403339

[33] H. Zhang, J. He, J. Qu. Metal-coordinated amino acid hydrogels with ultra-stretchability, adhesion, and self-healing properties for wound healing, Eur. Polym. J. 179 (2022) 111548, https://doi.org/10.1016/j.eurpolymj.2022.111548

[34] X.Q. Dou, C.L. Feng, Amino acids and peptide-based supramolecular hydrogels for three-dimensional cell culture, Adv. Mater. 29 (16) (2017) 1604062, https://doi.org/10.1002/adma.201604062

[35] J. Kang, S.I. Yun, Fmoc-phenylalanine as a building block for hybrid double network hydrogels with enhanced mechanical properties, self-recovery, and shape memory capability, Polymer. 255 (2022) 125145, https://doi.org/10.1016/j.polymer.2022.125145

[36] M. Qiu, D. Wang, W. Liang, L. Liu, Y. Zhang, X. Chen, D.K. Sang, C. Xing, Z. Li, B. Dong, F. Xing, D. Fan, S. Bao, H. Zhang, Y. Cao, Novel concept of the smart NIR-light-controlled dru

g release of black phosphorus nanostructure for cancer therapy, Proc. Natl. Acad. Sci. 115 (3) (2018) 501-506, https://doi.org/10.1073/pnas.171442111

[37] S. Pearson, J.A. del Campo, Lighting the path: light delivery strategies to activate photoresponsive biomaterials in vivo, Adv. Funct. Mater. 31 (50) (2021) 2105989, https://doi.org/10.1002/adfm.202105989

[38] C. Guilbaud-Chéreau, B. Dinesh, R. Schurhammer, D. Collin, A. Bianco, C. Ménard-Moyon, Protected amino acid-based hydrogels incorporating carbon nanomaterials for near-infrared irradiation-triggered drug release, ACS Appl. Mater. Interfaces. 11 (14) (2019) 13147-13157, https://doi.org/10.1021/acsami.9b02482

[39] J. Gong, Y. Katsuyama, T. Kurokawa, Y. Osada, Double-network hydrogels with extremely high mechanical strength, Adv. Mater. 15 (14) (2003) 1155-1158, https://doi.org/10.1002/adma.200304907

[40] X. Xu, V. Jerca, R. Hoogenboom, Bioinspired double network hydrogels: from covalent double network hydrogels via hybrid double network hydrogels to physical double network hydrogels, Mater. Horiz. 8 (4) (2021) 1173-1188, https://doi.org/10.1039/D0MH01514H

[41] D. Gan, T. Xu, T, W. Xing, X. Ge, L. Fang, K. Wang, X. Lu, Mussel-inspired contact-active antibacterial hydrogel with high cell affinity, toughness, and recoverability, Adv. Funct. Mater. 29 (1) (2019) 1805964, https://doi.org/10.1002/adfm.201805964

[42] X. Huang, J. Li, J. Luo, Q. Gao, A. Mao, J. Li, Research progress on double-network hydrogels, Mater. Today Commun. 29 (2021) 102757, https://doi.org/10.1016/j.mtcomm.2021.102757

[43] W. Dai, H. Guo, B. Gao, M. Ruan, L. Xu, J. Wu, W. Xue, Double network shape memory hydrogels activated by near-infrared with high mechanical toughness, nontoxicity, and 3D printability, Chem. Eng. J. 356 (2019) 934-949, https://doi.org/10.1016/j.cej.2018.09.078

[44] Y. Zhao, T. Nakajima, J. Yang, T. Kurokawa, J. Liu, J. Lu, J. Gong, Proteoglycans and glycosaminoglycans improve toughness of biocompatible double network hydrogels, Adv. Mater. 26 (3) (2014) 436-442, https://doi.org/10.1002/adma.201303387

[45] Q. Chen, H. Chen, L. Zhu, J. Zheng, Fundamentals of double network hydrogels, J. Mater. Chem. B. 3 (18) (12015) 3654-3676, https://doi.org/10.1039/C5TB00123D

[46] H. Xin. Double-network tough hydrogels: a brief review on achievements and challenges, Gels. 8 (4) (2022) 247, https://doi.org/10.3390/gels8040247

[47] M. Khodadadi Yazdi, A. Taghizadeh, M. Taghizadeh, F.J. Stadler, M. Farokhi, F. Mottaghitalab, P. Zarrintaj, J.D. Ramsey, F. Seidi, M.R. Saeb, M. Mozafari, Agarose-based biomaterials for advanced drug delivery, J. Control. Release. 326 (2020) 523-543, https://doi.org/10.1016/j.jconrel.2020.07.028

[48] K. J. Le Goff, C. Gaillard, H. Welbert, C. Garnier, & T. Aubry, Rheological study of reinforcement of agarose hydrogels by cellulose nanowhiskers. Carbohydr. Polym. 116 (2015) 117-123, https://doi.org/10.1016/j.carbpol.2014.04.085

[49] N. Zhang, J. Wang, J. Ye, P. Zhao, M. Xiao, Oxyalkylation modification as a promising method for preparing low-melting-point agarose, Int. J. Biol. Macromol. 117 (2018) 696-703, https://doi.org/10.1016/j.ijbiomac.2018.05.171

[50] L.M. Zhang, C.X. Wu, J.Y. Huang, X.H. Peng, P. Chen, S.Q. Tang, Synthesis and characterization of a degradable composite agarose/HA hydrogel, Carbohydr. Polym. 88 (4) (2012) 1445-1452, https://doi.org/10.1016/j.carbpol.2012.02.050

[51] M. El-Kady, A.A. Ali, A. El-Fiqi, Controlled delivery of therapeutic ions and antibiotic drug of novel alginate-agarose matrix incorporating selenium-modified borosilicate glass designed for chronic wound healing, J. Non-Cryst. Solids. 534 (2020) 119889, https://doi.org/10.1016/j.jnoncrysol.2020.119889

[52] C. Kim, D. Jeong, S. Kim, Y. Kim, S. Jung, Cyclodextrin functionalized agarose gel with low gelling temperature for controlled drug delivery systems, Carbohydr. Polym. 222 (2019) 115011, https://doi.org/10.1016/j.carbpol.2019.115011

[53] M. Pourmadadi, M. Ahmadi, M. Abdouss, F. Yazdian, H. Rashedi, M. Navaei-Nigjeh, Y. Hesari, The synthesis and characterization of double nanoemulsion for targeted co-delivery of 5-fluorouracil and curcumin using pH-sensitive agarose/chitosan nanocarrier, J. Drug Delivery Sci. Technol. 70 (2022) 102849, https://doi.org/10.1016/j.jddst.2021.102849

[54] F.A. Andersen, Amended final report on the safety assessment of polyacrylamide and acrylamide residues in cosmetics, Int. J. Toxicol. 24 (2005) 21-50, https://doi.org/10.1080/10915810590953

[55] M. A. Haq, Y. Su, D. Wang, Mechanical properties of PNIPAM based hydrogels: a review. Mater. Sci. Eng. C. 70 (2017) 842-855, https://doi.org/10.1016/j.msec.2016.09.081

[56] P. Wang, M. Wu, R. Li, Z. Cai, H. Zhang, Fabrication of a double-network hydrogel based on carboxymethylated curdlan/polyacrylamide with highly mechanical performance for cartilage r

epair, ACS Appl. Polym. Mater. 3 (11) (2021) 5857-5869, https://doi.org/10.1021/acsapm.1c01094

[57] A.D. Kasi, V. Pergialiotis, D.N. Perrea, A. Khunda, S.K. Doumouchtsis, Polyacrylamide hydrogel (Bulkamid®) for stress urinary incontinence in women: a systematic review of the literature, Int. Urogynecol. J. 27 (2016) 367-375, https://doi.org/10.1007/s00192-015-2781-y

[58] A. Halperin, M. Kröger, F.M. Winnik, Poly(*N*-isopropylacrylamide) phase diagrams: fifty years of research, Angew. Chem., Int. Ed. 54 (51) (2015) 15342-15367, https://doi.org/10.1002/anie.201506663

[59] S. Ashraf, H.K. Park, H. Park, S.H. Lee, Snapshot of phase transition in thermoresponsive hydrogel PNIPAM: role in drug delivery and tissue engineering, Macromol. Res. 24 (4) (2016) 297-304, https://doi.org/10.1007/s13233-016-4052-2

[60] M. Cao, Y. Wang, X. Hu, H. Gong, R. Li, H. Cox, J. Zhang, T.A. Waigh, H. Xu, J.R. Lu, Reversible Thermoresponsive peptide-PNIPAM hydrogels for controlled drug delivery, Biomacromolecules. 20 (9) (2019) 3601-3610, https://pubs.acs.org/doi/10.1021/acs.biomac.9b01009

[61] G. Chen, Y. Zhou, J. Dai, S. Yan, W. Miao, L. Ren, Calcium alginate/PNIPAAm hydrogel with body temperature response and great biocompatibility: application as burn wound dressing, Int. J. Biol. Macromol. 216 (2022) 686-697, https://doi.org/10.1016/j.ijbiomac.2022.07.019

[62] S. Rasib, Z. Ahmad, A. Khan, H. Akil, M. Othman, Z. Hamid, F. Ullah. Synthesis and evaluation on pH-and temperature-responsive chitosan-p(MAA-co-NIPAM) hydrogels, Int. J. Biol. Macromol. 108 (2018) 367-375, https://doi.org/10.1016/j.ijbiomac.2017.12.021

[63] C. Qian, Y. Li, C. Chen, L. Han, Q. Han, L. Liu, & Z. Lu. A stretchable and conductive desi gn based on multi-responsive hydrogel for self-sensing actuators. Chem. Eng. J. 454 (2023), 140 263, https://doi.org/10.1016/j.cej.2022.140263

[64] J. Lv, B. Sun, J. Jin, W. Jiang. Mechanical and slow-released property of poly(acrylamide) h ydrogel reinforced by diatomite, Mater. Sci. Eng., C. 99 (2019) 315-321, https://doi.org/10.1016/ j.msec.2019.01.109

[65] Z. Atoufi, S.K. Kamrava, S.M. Davachi, M. Hassanabadi, S.S. Garakani, R. Alizadeh, G.H. Motlagh, Injectable PNIPAM/hyaluronic acid hydrogels containing multipurpose modified partic les for cartilage tissue engineering: synthesis, characterization, drug release and cell culture study , Int. J. Biol. Macromol. 139 (2019) 1168-1181, https://doi.org/10.1016/j.ijbiomac.2019.08.101

[66] Lv, B. Lv, X. Bu, Y. Da, P. Duan, H. Wang, J. Ren, B. Lyu, D. Gao, J. Ma, Gelatin/PAM do uble network hydrogels with super-compressibility, Polymer. 210 (2020) 123021, https://doi.org/ 10.1016/j.polymer.2020.123021

[67] H. Jung, M.K. Kim, J.Y. Lee, S.W. Choi, J. Kim, Adhesive hydrogel patch with enhanced st rength and adhesiveness to skin for transdermal drug delivery, Adv. Funct. Mater. 30 (2020) 200 4407, https://doi.org/10.1002/adfm.202004407

[68] S. Xu, H. Li, H. Ding, Z. Fan, P. Pi, J. Cheng, X. Wen, Allylated chitosan-poly (*N*-isopropyl acrylamide) hydrogel based on a functionalized double network for controlled drug release, Carb ohydr. Polym. 214 (2019) 8-14, https://doi.org/10.1016/j.carbpol.2019.03.008

[69] H. Li, Y. Xie, X. Zou, Z. Li, W. Liu, G. Liu, Y. Zheng, Ultrasonic/electrical dual stimulation response nanocomposite bioelectret for controlled precision drug release, Mater. Today Bio 20 (2023) 100665, https://doi.org/10.1016/j.mtbio.2023.100665

[70] I. Marangon, C. Ménard-Moyon, J. Kolosnjaj-Tabi, M.L. Béoutis, L. Lartigue, D. Alloyeau, E. Pach, B. Ballesteros, G. Autret, T. Ninjbadgar, D.F. Brougham, A. Bianco, F. Gazeau, Covalent functionalization of multi-walled carbon nanotubes with a gadolinium chelate for efficient T_1-weighted magnetic resonance imaging, Adv. Funct. Mater. 24 (45) (2014) 7173-7186, https://doi.org/10.1002/adfm.201402234

[71] K.G. Zhou, N.N. Mao, H.X. Wang, Y. Peng, H.L. Zhang, A mixed-solvent strategy for efficient exfoliation of inorganic graphene analogues, Angew. Chem. Int. Ed. 50 (46) (2011) 10839-10842, https://doi.org/10.1002/anie.201105364

[72] P. Erkekoglu, T. Baydar, Acrylamide neurotoxicity, Nutr. Neurosci. 17 (2) (2014) 49-57, https://doi.org/10.1179/1476830513Y.0000000065

[73] Y. Komoike, M. Matsuoka, *In vitro* and *in vivo* studies of oxidative stress responses against acrylamide toxicity in zebrafish, J. Hazard. Mater. 365 (2019) 430-439, https://doi.org/10.1016/j.jhazmat.2018.11.023

[74] J. Ma, Y. Lin, Y.W. Kim, Y. Ko, J. Kim, K.H. Oh, J.Y. Sun, C.B. Gorman, M.A. Voinov, A.I. Smirnov, J. Genzer, M.D. Dickey, Liquid metal nanoparticles as initiators for radical polymerization of vinyl monomers, ACS Macro Lett. 8 (11) (2019) 1522-1527, https://doi.org/10.1021/acsmacrolett.9b00783

[75] L. Yu, J. Ding, Injectable hydrogels as unique biomedical materials, Chem. Soc. Rev. 37 (8) (2008) 1473-1481, https://doi.org/10.1039/B713009K

[76] D.J. Overstreet, D. Dutta, S.E. Stabenfeldt, B.L. Vernon, Injectable hydrogels, J. Polym. Sci ., Part B: Polym. Phys. 50 (13) (2012) 881-903, https://doi.org/10.1002/polb.23081

[77] T. Portnov, T.R. Shulimzon, M. Zilberman, Injectable hydrogel-based scaffolds for tissue en gineering applications, Rev. Chem. Eng. 33 (1) (2017) 91-107, https://doi.org/10.1515/revce-201 5-0074

[78] T.R. Hoare, D.S. Kohane, Hydrogels in drug delivery: progress and challenges, Polymer. 49 (8) (2008) 1993-2007, https://doi.org/10.1016/j.polymer.2008.01.027

[79] F. Rizzo, N.S. Kehr, Recent advances in injectable hydrogels for controlled and local drug d elivery, Adv. Healthc. Mater. 10 (1) (2021) 2001341, https://doi.org/10.1002/adhm.202001341

[80] C. Veerman, K. Rajagopal, C.S. Palla, D.J. Pochan, J.P. Schneider, E.M. Furst, Gelation kin etics of β-hairpin peptide hydrogel networks, Macromolecules. 39 (19) (2006) 6608-6614, https:/ /doi.org/10.1021/ma0609331

[81] H.C. Tseng, C.Y. Kuo, W.T. Liao, T.S. Chou, J.K. Hsiao, Indocyanine green as a near-infrar ed theranostic agent for ferroptosis and apoptosis-based, photothermal, and photodynamic cancer therapy, Front. Mol. Biosci. 9 (2022), 1045885, https://doi.org/10.3389/fmolb.2022.1045885

[82] M. Liu, H. Zhu, Y. Wang, C. Sevencan, B.L. Li, Functionalized MoS_2-based nanomaterials for cancer phototherapy and other biomedical applications, ACS Materials Lett. 3 (5) (2021) 462 -496, https://doi.org/10.1021/acsmaterialslett.1c00073

[83] V. Normand, D.L. Lootens, E. Amici, K.P. Plucknett, P. Aymard, New insight into agarose gel mechanical properties, Biomacromolecules. 1 (4) (2000), 730-738, https://doi.org/10.1021/bm005583j

[84] K. Bertula, L. Martikainen, P. Munne, S. Hietala, J. Klefström, O. Ikkala, Nonappa, Strain-stiffening of agarose gels, ACS Macro Lett. 8 (6) (2019) 670-675, https://doi.org/10.1021/acsmacrolett.9b00258

[85] N. de Sousa, D. Santos, S. Monteiro, N. Silva, A. Barreiro-Iglesias, A.J. Salgado, Role of baclofen in modulating spasticity and neuroprotection in spinal cord injury, J. Neurotrauma. 39 (3-4) (2022) 249-258, https://doi.org/10.1089/neu.2020.7591

[86] O.A. Savchuk, J.J. Carvajal, J. Massons, M. Aguiló, & F. Díaz, Determination of photothermal conversion efficiency of graphene and graphene oxide through an integrating sphere method. Carbon. 103 (2016) 134-141, https://doi.org/10.1016/j.carbon.2016.02.075

[87] L.M. Maestro, P. Haro-González, B. Del Rosal, J. Ramiro, A.J. Caamano, E. Carrasco, D. Jaque, Heating efficiency of multi-walled carbon nanotubes in the first and second biological windows. Nanoscale. 5 (17) (2013) 7882-7889, https://doi.org/10.1039/C3NR01398G

[88] J. Liu, K. Lu, F. Gao, L. Zhao, H. Li, Y. Jiang, Multifunctional MoS_2 composite nanomaterials for drug delivery and synergistic photothermal therapy in cancer treatment. Ceram. Int. 48 (15) (2022) 22419-22427, https://doi.org/10.1016/j.ceramint.2022.04.244

[89] H.J. Yoon, H.S. Lee, J.Y. Lim, & J.H. Park, Liposomal indocyanine green for enhanced photothermal therapy. ACS Appl. Mater. Interfaces. 9 (7) (2017) 5683-5691, https://doi.org/10.1021/acsami.6b16801

[90] S. Okuyama, T. Nagaya, F. Ogata, Y. Maruoka, K. Sato, Y. Nakamura, P.L. Choyke, H. Kobayashi, Avoiding thermal injury during near-infrared photoimmunotherapy (NIR-PIT): the importance of NIR light power density, Oncotarget. 8 (68) (2017) 113194-113201, https://doi.org/10.18632/oncotarget.20179

[91] L. Pan, J. Liu, J. Shi, Nuclear-targeting gold nanorods for extremely low NIR activated photothermal therapy, ACS Appl. Mater. Interfaces. 9 (19) (2017) 15952-15961, https://doi.org/10.1021/acsami.7b03017

[92] K. Yang, H. Xu, L. Cheng, C. Sun, J. Wang, Z. Liu, *In vitro* and *in vivo* near-infrared photothermal therapy of cancer using polypyrrole organic nanoparticles, Adv. Mater. 24 (41) (2012) 5586-5592, https://doi.org/10.1002/adma.201202625

[93] D. Kim, G. Jo, Y. Chae, S. Subramani, B.Y. Lee, E.J. Kim, M.K. Ji, U. Sim, H. Hyun, Bioinspired *Camellia japonica* carbon dots with high near-infrared absorbance for efficient photothermal cancer therapy, Nanoscale. 13 (34) (2021) 14426-14434, https://doi.org/10.1039/D1NR03999G

[94] D. Chouhan, T.U. Lohe, P.K. Samudrala, B.B. Mandal, *In situ* forming injectable silk fibroin hydrogel promotes skin regeneration in full thickness burn wounds, Adv. Healthc. Mater. 7 (24) (2018) 1801092, https://doi.org/10.1002/adhm.201801092

[95] T. De Serres-Berard, T.B. Becher, C.B. Braga, C. Ornelas, F. Berthod, Neuropeptide substance P released from a nonswellable laponite-based hydrogel enhances wound healing in a tissue-engineered skin *in vitro,* ACS Appl. Polym. Mater. 2 (12) (2020) 5790-5797, https://doi.org/10.1021/acsapm.0c01034

[96] Y.S. Chen, P.C. Tsou, J.M. Lo, H.C. Tsai, Y.Z. Wang, & G.H. Hsiue, Poly (*N*-isopropylacry lamide) hydrogels with interpenetrating multiwalled carbon nanotubes for cell sheet engineering. Biomaterials. 34 (30) (2013) 7328-7334, https://doi.org/10.1016/j.biomaterials.2013.06.017

[97] H. Yu, H. Zhao, C. Huang, & Y. Du, Mechanically and electrically enhanced CNT-collagen hydrogels as potential scaffolds for engineered cardiac constructs. ACS Biomater. Sci. Eng. 3 (1 1) (2017) 3017-3021, https://doi.org/10.1021/acsbiomaterials.6b00620

[98] X. Sun, Z. Qin, L. Ye, H. Zhang, Q. Yu, X. Wu, F. Yao, Carbon nanotubes reinforced hydro gel as flexible strain sensor with high stretchability and mechanically toughness. Chem. Eng. J. 3 82 (2020) 122832, https://doi.org/10.1016/j.cej.2019.122832

[99] H. Zhang, D. Zhai, & Y. He, Graphene oxide/polyacrylamide/carboxymethyl cellulose sodiu m nanocomposite hydrogel with enhanced mechanical strength: preparation, characterization and the swelling behavior. RSC Adv. 4 (84) (2014) 44600-44609, https://doi-org.scd-rproxy.u-strasb g.fr/10.1039/C4RA07576E

[100] J. Huang, L. Zhao, T. Wang, W. Sun, & Z. Tong, NIR-triggered rapid shape memory PAM -GO-gelatin hydrogels with high mechanical strength. ACS Appl. Mater. Interfaces. 8 (19) (2016) 12384-12392, https://doi.org/10.1021/acsami.6b00867

[101] K.M Lee, Y. Oh, H. Yoon, M. Chang, H. Kim, Multifunctional role of MoS_2 in preparation of composite hydrogels: radical initiation and cross-linking. ACS Appl. Mater. Interfaces. 12 (7) (2020) 8642-8649, https://doi.org/10.1021/acsami.9b19567

[102] Z. Zohreband, M. Adeli, A. Zebardasti, Self-healable and flexible supramolecular gelatin/ MoS_2 hydrogels with molecular recognition properties. Int. J. Biol. Macromol. 182 (2021) 2048-2055, https://doi.org/10.1016/j.ijbiomac.2021.05.106

[103] H.E. Jeleel, F.J. Jawad, Formulation and *in-vitro* evaluation of super porous hydrogel comp osite of baclofen, Int. J. Drug. Deliv. Technology. 11 (4) (2021) 1372-1378, https://doi.org/10.25258/ijddt.11.4.42